Adenosine triphosphate utilization rates and metabolic pool sizes in intact cells measured by transfer of ^{18}O from water

Stevan M. Dawis,* Timothy F. Walseth,‡ Mark A. Deeg,‡ Richard A. Heyman,‡ Richard M. Graeff,* and Nelson D. Goldberg*

Departments of Biochemistry* and Pharmacology,‡ University of Minnesota Medical School, Minneapolis, Minnesota 55455

ABSTRACT The hydrolytic rates and metabolic pool sizes of ATP were determined in intact cells by monitoring the time courses of ^{18}O incorporation from ^{18}O-water into the γ-phosphoryl of ATP and orthophosphate. To calculate the rate of ATP hydrolysis, a kinetic model is used to fit the time course of the ^{18}O labeling. The size of the metabolic pool of ATP is calculated from the ^{18}O distribution after isotopic equilibrium has been achieved. Metabolic pools have a binomial distribution of ^{18}O whereas nonmetabolic pools exhibit negligible ^{18}O labeling. The application and limitations of this approach are illustrated with data from isolated toad retinas and human platelets. At 22°C, the time constant of ATP hydrolysis in the dark-adapted toad retina is about 30 s. Under these conditions, over 80% of the retinal ATP is involved in high-energy phosphate metabolism. It is calculated that when cGMP metabolic flux in the photoreceptors is maximally stimulated by light, it accounts for 10% of the ATP utilization by the entire retina. The time constant of ATP hydrolysis in human platelets at 37°C is ~1 s, and 60% of the platelet ATP is involved in energy metabolism.

INTRODUCTION

The rate of ATP hydrolysis (and synthesis) is of paramount importance in the cellular metabolism of high-energy phosphates (Lipmann, 1941), yet direct methods of estimating this rate under physiological conditions have been difficult to achieve. In many metabolic studies, the issue of ATP hydrolytic rate is avoided and the energy economy of the cell is monitored by measuring the intracellular levels of high-energy phosphates. A hint of the dynamics underlying the cellular energy process is given by the time courses of disappearance of high-energy phosphates and substrates and the appearance of lactic acid during ischemia (Lowry et al., 1964). The metabolism of glucose, glycogen, and phosphocreatine, which temporarily sustains the ATP level, prevents an accurate determination of the rate of ATP hydrolysis by this method. Consequently, ATP hydrolytic rates have been estimated by inhibiting the synthesis of ATP (Winkler, 1981; Akkerman et al., 1983). However, regulatory mechanisms that tend to maintain the adenine energy charge of the cell distort these analyses, causing the rate of ATP utilization to be underestimated (Chapman and Atkinson, 1977).

Isotopic tracer methods are less likely to perturb the metabolic balance of the cell. For example, ^{32}P-labeled orthophosphate has been used to measure the cellular rate of ATP hydrolysis. This method requires that the radiolabeled orthophosphate added to the medium enters the cell and becomes incorporated into ATP upon phosphorylation of ADP. Although useful for measuring ATP hydrolytic rates in microbial cells (Karl and Bossard, 1985), this method is not applicable to most eukaryotic cells because transport of orthophosphate across the plasma membrane is slow and/or regulated.

^{31}P-nuclear magnetic resonance (NMR) spectroscopy is another technique that requires minimal perturbation for observing high-energy phosphate metabolism in intact cells. One advantage of this method is that the levels of only the mobile species of adenine and guanine nucleotides, orthophosphate, and phosphocreatine are observed. Another advantage is that the time course of changes in the levels of these molecules can be followed in a single tissue.^{31}P-NMR spectroscopy can be used to increase the sophistication of the earlier methods used to estimate ATP utilization. For example, it can be used to monitor the decline in free ATP and phosphocreatine in response to ischemia (Lee et al., 1987). Another example is the estimation of lactic acid production from intracellular pH changes monitored by the spectrum of orthophosphate (Dawson et al., 1978). However, the estimates of the rate of ATP utilization by these methods are still indirect. In contrast, the method of saturation transfer monitored by ^{31}P-NMR spectroscopy (Brown et al., 1977; Bittl and Ingwall, 1985) provides a direct measurement of the rate of ATP hydrolysis in intact cells. A constraint in this

Dr. Dawis's present address is The Rockefeller University, New York 10021.

Dr. Deeg's present address is Cleveland Metropolitan General Hospital, Cleveland, OH 44109.

Dr. Heyman's present address is The Salk Institute, San Diego, CA 92138.

Address reprint requests to Dr. Goldberg.

0006-3495/89/01/79/21 $2.00

methodology is the long period (nearly 1 h) necessary to acquire the spectral information used to measure metabolic time constants of less than 1 s (Bittl and Ingwall, 1985).

Quantitative information about ATP metabolism in an intact tissue or a suspension of cells can be obtained by measuring the rate of ^{18}O appearance in the γ-phosphoryl of ATP and orthophosphate upon incubation of the preparation in medium containing $H_2{}^{18}O$. (Incorporation of ^{18}O results from the processes of hydrolytic cleavage and phosphoryl transfer). With this measurement the only perturbation to the biological system is the rapid substitution of control medium with medium containing a higher percent excess of $H_2{}^{18}O$. Since intracellular water equilibrates rapidly with extracelluar water, this tracer isotope method is more generally applicable than a method that employs [^{32}P]orthophosphate. Measurements of metabolic flux by ^{18}O incorporation require incubations in the range of seconds to minutes and provide information about several metabolic pathways simultaneously.

The purpose of the present paper is to demonstrate that (*a*) the size of "metabolic pools" of high-energy phosphates can be calculated from the distribution of ^{18}O in tissue phosphoryls at isotopic equilibrium and (*b*) the rate of ATP hydrolysis can be determined from the time course of ^{18}O incorporation into high-energy phosphates. In this respect, the ^{18}O technology complements ^{31}P-NMR spectroscopy. Whereas ^{31}P-NMR spectroscopy detects molecular species that are mobile, the ^{18}O technology detects species that are available for metabolism during the incubation period with $H_2{}^{18}O$. The results obtained with these two different methods can be compared to determine the relationship between the metabolic pool and the mobile pool of molecules. In addition, the two methods independently provide direct measurements of the kinetics of ATP metabolism in intact cells. A first step in mathematically modeling the dynamical process of ^{18}O incorporation into the γ-phosphoryl of ATP and orthophosphate from ^{18}O-labeled water is presented. The use of this model to calculate ATP hydrolytic rate is illustrated with data from toad retinas and human platelets. An alternative model is used to determine a lower bound for the rate of synthesis of ATP from ADP in human platelets. The second model is based on the time courses of appearance of ^{18}O into the β-phosphoryls of ADP and ATP.

METHODS

Preparation and incubation of toad retinas

The protocol used for preparing and incubating dark-adapted, isolated toad retinas has been described previously (Dawis et al., 1988). After a retina had been dissected, it was allowed to equilibrate with oxygenated incubation medium for at least 15 min. Throughout this and the following incubations the retina was backlighted by a very dim red light. The medium was then replaced with medium containing ^{18}O-labeled water and incubated for a predetermined time interval (either 20, 40, 60, 120, 600, 1,800, or 3,600 s). The incubation in medium containing $H_2{}^{18}O$ was terminated by transferring the retina into 5 ml of ice-cold 0.5 M perchloric acid. Samples were processed for measurement of percent excess of ^{18}O in the γ-phosphoryl of ATP, orthophosphate, and medium water.

Preparation and incubation of platelets

General methods for the experiments with platelets have been described (Walseth et al., 1983). An important difference in protocol for the time course experiment shown in Figs. 4 and 5 is that phosphate-free buffer was used. This permitted the determination of ^{18}O incorporation into cellular orthophosphate without interference from medium phosphate. Human blood (Red Cross, type B, Rh^+), 98 ml volume, was centrifuged for 20 min at 900 *g* to remove red blood cells. The platelet-rich plasma was centrifuged at 3,000 *g* for 20 min. Pellets were resuspended in 35 ml of a modified Hank's balanced salt solution (HBSS) without phosphate: 5.4 mM KCl, 140 mM NaCl, 5.56 mM glucose, 0.5 mM EDTA; buffered with 25 mM HEPES and titrated with $NaHCO_3$ to pH 7.4; and oxygenated for 30 min. Incubation was begun by warming the platelet suspension to 37°C and adding 5 ml of the suspension to 5 ml of the incubation medium (77.91% enriched $H_2{}^{18}O$, HBSS without phosphate, 5 mM $CaCl_2$ at 37°C), resulting in a final concentration of 6.05×10^8 platelets/ml. Samples were incubated at 37°C with stirring. At 30, 60, 180, 360, and 600 s, a 2-ml aliquot was removed and quenched with 90 μl of 11.65 M perchloric acid. Samples were processed for measurement of percent excess of ^{18}O into the β-phosphoryls of ADP and ATP, the γ-phosphoryl of ATP, orthophosphate, and medium water. A similar procedure was used for the other experiments with platelets listed in Table 1, except that HBSS with phosphate (0.44 mM KH_2PO_4 and 0.34 mM $Na_2HPO_4 \cdot 7H_2O$) was used.

Determination of ^{18}O incorporation

The procedure for measurement of the atom percent excess of ^{18}O in the β-phosphoryls of ADP and ATP, the γ-phosphoryl of ATP, and orthophosphate have been described previously (Walseth et al., 1983, 1988). After extraction with perchloric acid, the adenine nucleotides and orthophosphate are separated by boronate chromatography and high performance liquid chromatography. The γ- and β-phosphoryl groups are enzymically transferred to glycerol-3-phosphate and chromatographically separated. Orthophosphate and glycerol-3-phosphate samples are trimethylsilylated and analyzed by gas chromatography/mass spectrometry to determine isotope ratios.

Computer modeling

Kinetic models were implemented by STELLA® (High Performance Systems Lyme, NH) on a Macintosh II (Apple Computer, Cupertino, CA). The program solved the differential equations by using the four-order Runge-Kutta method with the following time increments: $dt = 0.125$ s for Figs. 3 and 5 and $dt = 0.0125$ s for Fig 4.

RESULTS

The gamma model

The following is a description of a model for ^{18}O labeling of the γ-phosphoryl of ATP and orthophosphate. It is assumed that the simple mass action relationships diagrammed in Fig. 1 *A* are in effect. Specifically, it is assumed that the change in the concentration of ATP is given by

$$d[ATP]/dt = -k_{TD}[ATP] + k_{DT}[\text{orthophosphate}][ADP], \quad (1)$$

where [ATP] is the concentration (millimolar) of ATP at time t, [ADP] is the concentration (millimolar) of ADP at time t, [orthophosphate] is the concentration (millimolar) of inorganic orthophosphate at time t, k_{TD} is the rate constant (1 per second) of hydrolysis of ATP to ADP, and k_{DT} is the rate constant (1 per millimolar per second) of phosphorylation of ADP to ATP. Under steady-state conditions, the concentration of ATP does not change, in other words, $d[ATP]/dt = 0$, and consequently

$$k_{TD}[ATP] = k_{DT}[\text{orthophosphate}][ADP]. \quad (2)$$

In the following, it is assumed that the biological system has been allowed to attain the above steady-state condition. Under the steady-state condition, if the intracellular water is replaced entirely with $H_2{}^{18}O$, the hydrolysis of ATP to ADP will result in the incorporation of an ^{18}O atom into the inorganic orthophosphate product (Koshland and Clarke, 1953). The other product, ADP, will remain unlabeled. When an ADP molecule is phosphorylated with the newly ^{18}O-labeled phosphate, there is a 0.75 probability that an ATP molecule will be formed that has an ^{18}O in its γ-phosphoryl and a 0.25 probability that an unlabeled ATP molecule will be formed. These probabilities arise because phosphorylation will remove one of the four oxygen atoms of the labeled phosphate, of which three are ^{16}O and one ^{18}O. When an ATP molecule with one ^{18}O in its γ-phosphoryl is formed and then undergoes hydrolysis in medium containing 100 atom percent-enriched $H_2{}^{18}O$, an orthophosphate containing two atoms of ^{18}O will be formed. When the doubly labeled phosphate is used to phosphorylate an ADP molecule, there will be a 0.5 probability that the γ-phosphoryl group of the resulting ATP molecule will be singly labeled and a 0.5 probability that it will be doubly labeled. In this manner, ATP and orthophosphate molecules incorporate ^{18}O. It is possible to insert a maximum of three ^{18}O atoms into the γ-phosphoryl of ATP and a maximum of four into orthophosphate. The process asymptotically approaches a state of isotopic equilibrium in which all ATP and orthophosphate molecules are maximally labeled. If only a fraction of the water had been replaced with $H_2{}^{18}O$, the isotopic equilibrium would be characterized by ATP and orthophosphate molecules labeled to various extents: some labeled once, some twice, some three times and, in the case of inorganic phosphate, some four times. The observed distributions of ^{18}O labeling in the various phosphoryls at isotopic equilibrium will be shown to be binomial distributions. With this mathematical description of isotopic equilibrium, a determination can be made of the fraction of the cellular ATP that is in the metabolic pool (i.e., in the pool that is hydrolyzed or in pools that are rapidly exchangeable with the hydrolyzable pool). A mathematical description of how this process of ^{18}O incorporation approaches isotopic equilibrium will also be derived. This kinetic description provides a measure of the rate of ATP hydrolysis in the cell under the prevailing "steady state" condition.

A. Chemical Kinetics for Gamma Model

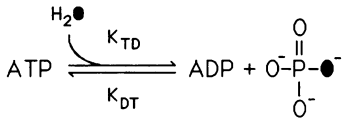

B. Chemical Kinetics for Beta Model

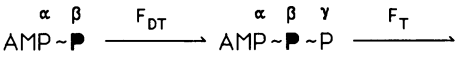

FIGURE 1. (*A*) Partial schematic diagram of the gamma model used for calculation of the rate of ATP hydrolysis by ^{18}O incorporation into the γ-phosphoryl of ATP and orthophosphate. The diagram illustrates a first approximation to the kinetics of ATP hydrolysis in intact cells. Parameters k_{TD} and k_{DT} are the rate constants for ATP hydrolysis and ADP phosphorylation, respectively. This kinetic model is combined with a probabilistic model of ^{18}O incorporation into and removal from phosphoryls. The first step in this probabilistic model, the incorporation of ^{18}O into orthophosphate upon hydrolysis of ATP, is shown. Subsequent steps are outlined in Results. The resulting hybrid model is used to reproduce the time course of ^{18}O labeling of the γ-phosphoryl of ATP and orthophosphate under steady-state conditions. Provided that the analysis is restricted to steady-state conditions, a simplified version of the kinetic model will yield the same results (see Appendix, first section). (*B*) Schematic diagram of the beta model used for calculation of the rate of ATP utilization by monitoring the conversion of ADP molecules with labeled β-phosphoryls to ATP molecules with labeled β-phosphoryls. In theory, this model is capable of providing an exact determination of the rate of ATP synthesis in intact cells (under steady-state conditions, this rate is equal to the rate of ATP utilization). In practice, as discussed in Results, ATP synthesis (utilization) is too rapid to be monitored in this manner. However, the beta model can be used to determine the upper limit of the time constant of ATP synthesis (utilization).

To construct the model, the following functions of time are defined: $w^*(t)$ = the fraction of intracellular water containing ^{18}O at time t; $D(t)$ = concentration (millimolar) of ADP, at time t; $T_j(t)$ = the concentration (millimolar) of ATP with j ^{18}O atoms in the γ-phosphoryl at time t, with $j = 0, 1, 2$, or 3; $P_k(t)$ = the concentration (millimolar) of orthophosphate with k ^{18}O atoms at time t, with $k = 0, 1, 2, 3$, or 4. By definition, $1 - w^*(t)$ is equal to the fraction of intracellular water containing ^{16}O at time t. Since it is assumed that the biological system is allowed to reach a steady-state condition before the incubation with ^{18}O-labeled water, each of the total concentrations of ADP, ATP, and orthophosphate will remain constant during the incubation. These constancies are expressed in the following constraints: at any time, t,

$$D(t) = \bar{D}, \tag{3.1}$$

$$\sum_{j=0}^{3} T_j(t) = \bar{T}, \tag{3.2}$$

$$\sum_{k=0}^{4} P_k(t) = \bar{P}, \tag{3.3}$$

where $\bar{D}$, $\bar{T}$, and $\bar{P}$ are the total concentrations of ADP, ATP, and orthophosphate, respectively, throughout the entire $H_2{}^{18}O$ incubation period. Since the system is assumed to be in a steady state, these concentrations are time invariant and are related as described in Eq. (2):

$$k_{TD}\bar{T} = k_{DT}\bar{P}\bar{D}. \tag{3.4}$$

The model for ^{18}O incorporation into the γ-phosphoryl of ATP and into orthophosphate is constructed by combining the law of mass action, as in Eq. (1), with the probabilities associated with ^{18}O incorporation. The equations are

$$dT_0/dt = -k_{TD}T_0 + k_{DT}(1.00\,P_0 + 0.25\,P_1)\bar{D} \tag{4.1}$$

$$dT_1/dt = -k_{TD}T_1 + k_{DT}(0.75\,P_1 + 0.50\,P_2)\bar{D} \tag{4.2}$$

$$dT_2/dt = -k_{TD}T_2 + k_{DT}(0.50\,P_2 + 0.75\,P_3)\bar{D} \tag{4.3}$$

$$dT_3/dt = -k_{TD}T_3 + k_{DT}(0.25\,P_3 + 1.00\,P_4)\bar{D} \tag{4.4}$$

$$dP_0/dt = k_{TD}\{1 - w^*\}T_0 - k_{DT}P_0\bar{D} \tag{4.5}$$

$$dP_1/dt = k_{TD}(w^*T_0 + \{1 - w^*\}T_1) - k_{DT}P_1\bar{D} \tag{4.6}$$

$$dP_2/dt = k_{TD}(w^*T_1 + \{1 - w^*\}T_2) - k_{DT}P_2\bar{D} \tag{4.7}$$

$$dP_3/dt = k_{TD}(w^*T_2 - \{1 - w^*\}T_3) - k_{DT}P_3\bar{D} \tag{4.8}$$

$$dP_4/dt = k_{TD}w^*T_3 - k_{DT}P_4\bar{D}. \tag{4.9}$$

The notation "(t)" has been dropped in the above and remaining equations to simplify the text.

A potential limitation of the model given by Eqs. (3.1) to (3.4) and (4.1) to (4.9) is that the model is restricted to the biochemical reactions in Fig. 1 *A*. For example, according to this scheme orthophosphate incorporates ^{18}O solely by ATP hydrolysis: see Eqs. (4.6) to (4.9). However, orthophosphate can also incorporate ^{18}O through GTPase activity. In addition, exchange of ^{18}O between water and orthophosphate mediated by pyrophosphatase has been observed in a cell-free system (Hackney and Boyer, 1978; Hackney, 1980). In Fig. 1 *A*, the γ-phosphoryl of ATP is shown to exchange only with orthophosphate. The γ-phosphoryl of ATP can, however, be transferred to creatine, GDP, or other molecules and can be cleaved along with the β-phosphoryl as pyrophosphate. Another restriction is that in the scheme in Fig. 1 *A* only one oxygen atom from water is incorporated into orthophosphate upon the hydrolysis of an ATP molecule. Multiple reversals of the hydrolytic reaction before the release of ADP and orthophosphate from the catalytic site of an ATPase have resulted in the incorporation of more than one medium oxygen under cell-free conditions (for myosin or myosin subfragment 1—Levy and Koshland, 1959; Shukla and Levy, 1977; and Sleep et al., 1978; for sarcoplasmic reticulum ATPase—Boyer et al., 1977). In chemically skinned muscle fibers, the pattern of ^{18}O labeling is consistent with two pathways of ATP hydrolysis, one with a low rate and a second with a high rate of multiple reversals (Hibberd *et al.*, 1985; Lund *et al.*, 1987). However, it is not known to what extent ATPases in intact cells undergo multiple reversals. This topic will be reexamined in the Discussion. In conclusion, a critical assumption of the model is that the biochemical reactions illustrated in Fig. 1 *A* represent the overwhelmingly fastest reactions in which ATP and orthophosphate are involved. If this is the case, the model will give a good approximation to reality.[1] In particular, the steady-state condition will be closely approximated by Eq. (3.4) and the model will provide a good estimate of the ATP hydrolytic rate based on the time course of ^{18}O incorporation.

Metabolic pool sizes determined from the ^{18}O distribution at isotopic equilibrium

The first goal is to describe mathematically the isotopic equilibrium that is approached after prolonged $H_2{}^{18}O$ incubation. The isotopic equilibrium equations are obtained by setting the derivatives in Eqs. (4.1) to (4.9) equal to zero (and setting $t = \infty$). The resulting nine linear equations can the be solved, with the aid of constraints

[1] A third implicit assumption is that the enzymes catalyzing the reactions in Fig. 1 *A* are operating well below saturation in a linear range. However, this assumption is optional since only steady-state behavior is being modeled (see Appendix, first section).

(3.1) to (3.4) for $T_0(\infty)$, . . . , $T_3(\infty)$, $P_0(\infty)$, . . . , $P_3(\infty)$, and $P_4(\infty)$. The values of $T_0(\infty)$ to $T_3(\infty)$ describe the distribution of ATP labeling at isotopic equilibrium (for example, $T_0(\infty)$ is equal to the concentration of ATP that is unlabeled at isotopic equilibrium). Similarily, the values of $P_0(\infty)$ to $P_4(\infty)$ describe the distribution of ^{18}O label in orthophosphate at isotopic equilibrium. The solution of the isotopic equilibrium equation is

$$\frac{T_j(\infty)}{\bar{T}} = \frac{3!}{(3-j)!j!}\{1 - w^*(\infty)\}^{3-j}\{w^*(\infty)\}^j, \quad \text{for } j = 0, 1, 2, \text{or } 3 \qquad (5.1)$$

$$\frac{P_k(\infty)}{\bar{P}} = \frac{4!}{(4-k)!k!}\{1 - w^*(\infty)\}^{4-k}\{w^*(\infty)\}^k, \quad \text{for } k = 0, 1, 2, 3, \text{or } 4. \qquad (5.2)$$

It can be verified that this is the solution to the isotopic equilibrium equations by substituting the expressions (5.1) and (5.2) into the right-hand side of Eqs. (4.1) to (4.9) and, with the aid of Eq. (3.4), demonstrating that the derivatives become equal to zero. Therefore, at isotopic equilibrium the ATP distribution, given by Eq. (5.1), and orthophosphate distribution, given by Eq. (5.2), are binomial distributions. This result is consistent with the premise that each oxygen atom in the γ-phosphoryl of ATP and each oxygen atom in orthophosphate has the probability $w^*(\infty)$ of being labeled with ^{18}O (and a probability $1 - w^*(\infty)$ of being ^{16}O) and that the isotopic species occupying any given oxygen position is independent of the isotopic species occupying the other positions in the same molecule. The ATP and orthophosphate distributions at isotopic equilibrium depend on $w^*(\infty)$, the fraction of intracellular water that is $H_2{}^{18}O$ at isotopic equilibrium. This dependence is illustrated in Fig. 2.

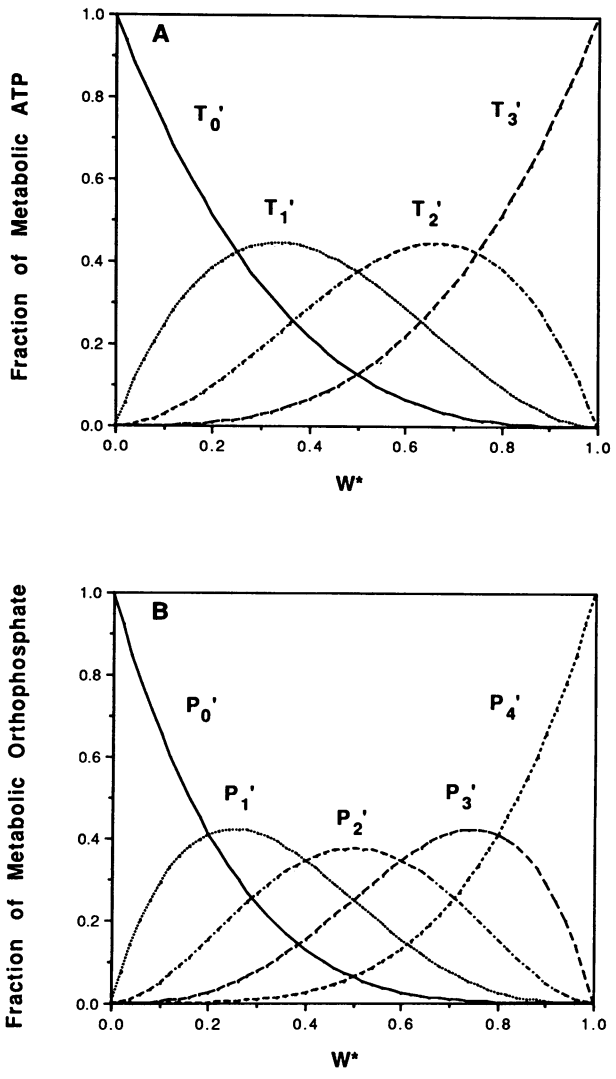

FIGURE 2 Theoretical distribution of ^{18}O at isotopic equilibrium in the γ-phosphoryl of ATP and orthophosphate as a function of w^*, the fraction of the intracellular water that is $H_2{}^{18}O$. (*A*) Fractions of ATP in the metabolic pool with zero, one, two, or three ^{18}O atoms in the γ-phosphoryl. These fractions are designated in the graph by T'_0, T'_1, T'_2, and T'_3, respectively. (*B*)Fractions of orthophosphate in the metabolic pool with zero, one, two, three, or four ^{18}O atoms. These fractions are designated in the graph by P'_0, P'_1, P'_2, P'_3, and P'_4, respectively. The distributions of ^{18}O at isotopic equilibrium are given by binomial distributions as predicted by assuming that the probability that a given exchangeable oxygen site is occupied by an ^{18}O is equal to w^* and that this probability is independent for each site. Since the theoretical distributions in *A* and *B* arise from the probabilistic and not the kinetic properties of the model, the distributions are independent of the specific kinetics assumed.

The mathematical description of the isotopic equilibrium can be used to determine what fraction of the ATP in the biological system is involved in reactions that result in the metabolism of the γ-phosphoryl of ATP. In the following, this fraction of ATP will be referred to as belonging to the "metabolic pool." To measure the metabolic pool of ATP, the biological system is incubated with a known fraction of $H_2{}^{18}O$, and after isotopic equilibrium is achieved, the distribution of ^{18}O labeling of the γ-phosphoryl of ATP is measured. If the ATP distribution at isotopic equilibrium is described by the binomial distribution given by Eq. (5.1), then all of the ATP belongs to the metabolic pool. If the binomial distribution does not describe the ATP distribution at isotopic equilibrium, the following modified binomial distribution could apply.

$$T_0(\infty)/\bar{T} = \{1 - w^*(\infty)\}^3 f_{\text{metabolic}} + f_{\text{nonmetabolic}} \qquad (6.1)$$

$$T_1(\infty)/\bar{T} = 3\{1 - w^*(\infty)\}^2\{w^*(\infty)\} f_{\text{metabolic}} \qquad (6.2)$$

$$T_2(\infty)/\bar{T} = 3\{1 - w^*(\infty)\}\{w^*(\infty)\}^2 f_{\text{metabolic}} \qquad (6.3)$$

$$T_3(\infty)/\bar{T} = \{w^*(\infty)\}^3 f_{\text{metabolic}}, \qquad (6.4)$$

where $f_{\text{metabolic}}$ and $f_{\text{nonmetabolic}}$ are the fractions of the entire

ATP content of the biological system that belong to the metabolic and nonmetabolic pools, respectively. For completeness, the following equation must be added to the above equations:

$$f_{\text{metabolic}} + f_{\text{nonmetabolic}} = 1. \quad (6.5)$$

The derivation of the distribution of ^{18}O at isotopic equilibrium depends only on the probabilistic properties and not the kinetic properties of the model. Therefore, the validity of using the modified binomial distribution to calculate the metabolic pool size is not conditional on the reaction kinetics shown in Fig. 1 *A*.

Eqs. (6.1) to (6.5) can be applied to the experimental data listed in Table 1. The first system is a dark-adapted, isolated toad retina which was incubated in 45% $H_2{}^{18}O$ for 60 min. The observed distribution of ^{18}O in the γ-phosphoryl of ATP is given in the second column of Table 1 (for example, 34.60% of the total ATP contained one ^{18}O atom in the γ-phosphoryl). The far right column shows the theoretical ATP distribution at isotopic equilibrium obtained from Eqs. (6.1) to (6.5) when $w^*(\infty)$ is set to 0.428 and $f_{\text{metabolic}}$ is set to 0.82. The theoretical values closely approximate the experimental values. This indicates that the intracellular water in the experiment attained an enrichment of 42.8% $H_2{}^{18}O$ and that 82% of the ATP content of the retinal system belonged to the metabolic pool. By contrast, only 60% of the ATP in the platelet preparations studied belonged to the metabolic pool. The second set of data in Table 1 was obtained from platelets that were incubated for 45 min in 43.9% $H_2{}^{18}O$, as determined by dilution. The measured distribution deviates significantly from a binomial distribution based on this atom percent enrichment of ^{18}O-water. However, the data fit very well the theoretical distribution generated by setting $w^*(\infty) = 0.408$ and $f_{\text{metabolic}} = 0.62$ in Eqs. (6.1) to (6.5). This theoretical distribution is given in Table 1. It is concluded that the intracellular water had been enriched to 40.8% $H_2{}^{18}O$ and that 62% of the total ATP belonged to the metabolic pool. Similar values for the size of the ATP metabolic pool were obtained with shorter incubation times (20 and 10 min). The observed and theoretical ^{18}O distributions for these two cases are also given in Table 1.

The mathematical description of the distribution of ^{18}O labeling of the γ-phosphoryl of ATP at isotopic equilibrium provides a means of determining the fraction of ATP that belongs to the metabolic pool (and also the fraction of intracellular water that is $H_2{}^{18}O$). However, the description of the labeling distribution at isotopic equilibrium given by Eqs. (6.1) to (6.5) yields no information about the rate of ATP hydrolysis. Information about the ATP hydrolytic rate is contained in the dynamic Eqs. (4.1) to (4.9) and constraining Eqs. (3.1) to (3.4). These equations describe the time course of ^{18}O incorporation into the γ-phosphoryl of ATP and into orthophosphate. The rate of ^{18}O incorporation will be related to the rate of ATP hydrolysis because Eqs. (4.1) to (4.9) contain the parameter k_{TD}, the rate constant for ATP hydrolysis. Even

TABLE 1 Comparison of the modified binomial distribution with the observed distributions of ^{18}O in γ-phosphoryl of ATP at isotopic equilibrium

Biological system and incubation time	^{18}O distribution in γ-phosphoryl of ATP	Theoretical system Eqs. (6.1) to (6.5)	Theoretical distribution at isotopic equilibrium
Dark-adapted retina incubated for 60 min in ~45% $H_2{}^{18}O$	$T_0/\bar{T} = 0.3318$	$w^* = 0.428$,	0.3335
	$T_1/\bar{T} = 0.3460$	$f_{\text{metabolic}} = 0.82$	0.3445
	$T_2/\bar{T} = 0.2584$		0.2578
	$T_3/\bar{T} = 0.0637$		0.0643
Platelets incubated for 45 min in ~43.9% $H_2{}^{18}O$	$T_0/\bar{T} = 0.5081$	$w^* = 0.408$,	0.5086
	$T_1/\bar{T} = 0.2660$	$f_{\text{metabolic}} = 0.62$	0.2660
	$T_2/\bar{T} = 0.1836$		0.1833
	$T_3/\bar{T} = 0.0423$		0.0421
Platelets incubated for 20 min in ~38.3% $H_2{}^{18}O$	$T_0/\bar{T} = 0.5534$	$w^* = 0.353$,	0.5552
	$T_1/\bar{T} = 0.2721$	$f_{\text{metabolic}} = 0.61$	0.2704
	$T_2/\bar{T} = 0.1486$		0.1475
	$T_3/\bar{T} = 0.0364$		0.0268
Platelets incubated for 10 min in ~39% $H_2{}^{18}O$	$T_0/\bar{T} = 0.6072$	$w^* = 0.323$,	0.6069
	$T_1/\bar{T} = 0.2531$	$f_{\text{metabolic}} = 0.57$	0.2531
	$T_2/\bar{T} = 0.1210$		0.1208
	$T_3/\bar{T} = 0.0187$		0.0192

Procedure for choosing values for w^* and $f_{\text{metabolic}}$ to fit the data with the modified binomial model: calculate the ratio of $T_1/\bar{T}$ to $T_2/\bar{T}$, according to Eqs. (6.2) and (6.3), this ratio is equal to $\{1\text{-}w^*\}/w^*$; therefore, set w^* equal to the inverse of one plus this ratio; with this value of w^*, quotients $(T_1/\bar{T})/3\{1\text{-}w^*\}^2w^*$ and $(T_2/\bar{T})/3\{1\text{-}w^*\}w^{*2}$ are equal to the same fraction; as can be derived from Eqs. (6.2) and (6.3) this fraction is $f_{\text{metabolic}}$. The theoretical distributions are obtained by substituting these calculated values of w^* and $f_{\text{metabolic}}$ into Eqs. (6.1) to (6.5).

without the mathematical description it is intuitively obvious that the faster the rate of hydrolysis, the faster will be the rate of ^{18}O incorporation. The goal of the next section is to recast Eqs. (4.1) to (4.9) into a form that more clearly expresses the properties of the gamma model.

Rate of ATP hydrolysis determined from the time course of ^{18}O incorporation

An implicit assumption underlying Eqs. (3.1) to (3.4) and (4.1) to (4.9) is that all molecules belong to the metabolic pool. It is evident from the preceding analysis of the distribution of ^{18}O in the γ-phosphoryl of ATP at isotopic equilibrium that some biological systems possess a significant portion of nonmetabolic ATP. In such cases, the nonmetabolic fraction must be subtracted from the total, and Eqs. (3.1) to (3.4) and (4.1) to (4.9) must be restricted to the metabolic pool. The latter procedure means that the definitions made earlier must be qualified. For example, $T_1(t)$ is replaced by $[ATP_{1,metabolic}(t)]$ = the concentration of ATP in the metabolic pool with one atom of ^{18}O in the γ-phosphoryl at time t and $\overline{T}$ is replaced by $[ATP_{metabolic}]$ = the concentration of ATP in the metabolic pool during the $H_2{}^{18}O$ incubation period. This presents a problem: to compare the mathematical model, as it is now stated, with experimental data, the absolute concentrations of ATP and orthophosphate in the metabolic pool must be determined. This problem can be circumvented by rewriting the equations in terms of fractions of the metabolic pool labeled. For example, $[ATP_{1,metabolic}(t)]/[ATP_{metabolic}]$ = the fraction of ATP in the metabolic pool with one atom of ^{18}O in the γ-phosphoryl at time t. The rewritten equations are[2]:

$$\alpha dT'_0/dt = -T'_0 + 1.00\,P'_0 + 0.25\,P'_1 \quad (7.1)$$

$$\alpha dT'_1/dt = -T'_1 + 0.75\,P'_1 + 0.50\,P'_2 \quad (7.2)$$

$$\alpha dT'_2/dt = -T'_2 + 0.50\,P'_2 + 0.75\,P'_3 \quad (7.3)$$

$$\alpha dT'_3/dt = -T'_3 + 0.25\,P'_3 + 1.00\,P'_4 \quad (7.4)$$

$$\alpha\beta dP'_0/dt = \{1 - w^*\}T'_0 - P'_0 \quad (7.5)$$

$$\alpha\beta dP'_1/dt = w^*T'_0 + \{1 - w^*\}T'_1 - P'_1 \quad (7.6)$$

$$\alpha\beta dP'_2/dt = w^*T'_1 + \{1 - w^*\}T'_2 - P'_2 \quad (7.7)$$

$$\alpha\beta dP'_3/dt = w^*T'_2 + \{1 - w^*\}T'_3 - P'_3 \quad (7.8)$$

$$\alpha\beta dP'_4/dt = w^*T'_3 - P'_4, \quad (7.9)$$

where

$$T'_j(t) = [ATP_{j,metabolic}(t)]/[ATP_{metabolic}] \quad \text{for } j = 0, 1, 2, \text{or } 3 \quad (7.10)$$

$$P'_k(t) = [orthophosphate_{k,metabolic}(t)]/[orthophosphate_{metabolic}] \quad \text{for } k = 0, 1, 2, 3, 4 \quad (7.11)$$

$$\alpha = 1/k_{TD} \quad (7.12)$$

$$\beta = [orthophosphate_{metabolic}]/[ATP_{metabolic}]. \quad (7.13)$$

In Eqs. (7.1) to (7.9) the notation (t) was omitted to simplify the text. Two constraints, the equivalents of Eqs. (3.2) and (3.3), are

$$\sum_{j=0}^{3} T'_j(t) = 1, \quad (7.14)$$

$$\sum_{k=0}^{4} P'_k(t) = 1. \quad (7.15)$$

To reiterate, $T'_j(t)$ is the fraction of ATP in the metabolic pool that contains j atoms of ^{18}O in the γ-phosphoryl at time t; $P'_k(t)$ is the fraction of orthophosphate in the metabolic pool that contains k atoms of ^{18}O at time t; k_{TD} is the rate constant of ATP hydrolysis as illustrated in Fig. 1 *A*; and $[orthophosphate_{metabolic}]/[ATP_{metabolic}]$ is the ratio of the concentration of orthophosphate to the concentration of ATP in the metabolic pool (if the volumes of the ATP and orthophosphate metabolic pools are equal, then measurements of amounts rather than concentrations are sufficient to calculate this ratio). For simplicity, assume that at $t = 0$ the water in the biological system is instantaneously replaced with water enriched by a fraction w^* with $H_2{}^{18}O$. In this case, w^* in Eqs. (7.5) to (7.9) is a constant rather than a time-varying function.

Eqs. (7.1) to (7.9) may appear to be as complex as Eqs. (4.1) to (4.9), but they are simpler. First, the equations are written in terms of the fractions of ATP and orthophosphate labeled to various extents with ^{18}O (these fractions are defined by Eqs. (7.10) and (7.11), respectively). Consequently, the model can be used without having to determine absolute concentrations of substrates

[2]Begin simplifying the model by dividing both sides of Eqs. (4.1) to (4.9) by the quantity $k_{TD}\overline{T}$, in the following way:

(*i*) after dividing the left-hand side of Eqs. (4.1) to (4.4), bring the term $\overline{T}$ into the derivative, that is, $(1/k_{TD}\overline{T})\,dT_j/dt$ becomes $(1/k_{TD})\,d\,(T_j/\overline{T})/dt$ for $j = 0, 1, 2,$ or 3;

(*ii*) in addition to dividing the left-hand side of Eqs. (4.5) to (4.9) by $k_{TD}\overline{T}$, multiply each derivative by $\overline{P}/\overline{P}$, which is unity, and bring the $\overline{P}$ in the denominator into the derivative, that is, $(1/k_{TD}\overline{T})\,(\overline{P}/\overline{P})\,dP_k/dt$ becomes $(1/k_{TD}\overline{T})\,\overline{P}d\,(P_k/\overline{P})/dt$ for $k = 0, 1, 2, 3,$ or 4;

(*iii*) on the right-hand side of Eqs. (4.1) to (4.9):

(*a*) all products containing the term k_{TD} are divided by $k_{TD}\overline{T}$, and

(*b*) all products containing the term k_{DT} are divided by $k_{DT}\overline{P}\overline{D}$ which, by Eq. (3.4), is equivalent to dividing by $k_{TD}\overline{T}$.

These manipulations result in Eqs. (7.1) to (7.9) with definitions (7.10) to (7.13).

in the metabolic pool. Second, there are only three parameters: α, β, and w^*. The model can be immediately reduced to two parameters since w^* can be determined from the ^{18}O distribution at isotopic equilibrium. Eqs. (7.1) to (7.9) can be used to generate theoretical curves that can be fit to experimental data by varying parameters α and β. Alternatively, Eqs. (7.1) to (7.9) can be further condensed and transformed into a form that is amenable to optimization algorithms for estimation of α and β (see Appendix, second section). In certain cases, a value for β can be determined by measurements of $[ATP_{metabolic}]$ and $[orthophosphate_{metabolic}]$. With direct measurements of w^* and β the set of Eqs. (7.1) to (7.9) becomes a model with a single parameter, α.

Application of the gamma model to data from toad retinas and human platelets

Two methods of applying the gamma model to experimental data are demonstrated in this section. Theoretical curves generated by the gamma model, Eqs. (7.1) to (7.15), are fitted to the data by choosing values for parameters w^*, α, and β. A value for w^* can be determined by fitting the observed distribution of ^{18}O in the γ-phosphoryl of ATP at isotopic equilibrium with the modified binomial distribution, Eqs. (6.1) to (6.5); therefore, only values for parameters α and β remain to be determined by application of the gamma model. In the example given with data from toad retinas, the method is to measure experimentally the ratio $[orthophosphate_{metabolic}]/[ATP_{metabolic}]$ which, by definition, is β. The time course of ^{18}O incorporation into the γ-phosphoryl of ATP is then fit by selecting a value of α. The method illustrated with data from human platelets is to choose values for α and β to fit the time courses of ^{18}O incorporation into the γ-phosphoryl of ATP and orthophosphate.

The data from dark-adapted toad retinas at 22°C are listed in the upper half of Table 2 in terms of fractions of the entire pool of ATP containing zero, one, two, or three atoms of ^{18}O in the γ-phosphoryl. In the lower half of Table 2 these data are expressed in terms of fractions of the metabolic pool of ATP. The procedure used for converting the data from the former to the latter format is outlined in Table 2. As mentioned earlier, the data must be presented in the latter format in order to apply the gamma model. The converted values are plotted in Fig. 3. From the ^{18}O distribution at isotopic equilibrium for this experiment, it was calculated that the intracellular water was enriched to 42.8% ^{18}O-water (Table 1). This sets the value for parameter w^* of the gamma model to 0.428. The retinal content of ATP was 15 nmol · mg protein^{-1}, and from the isotopic equilibrium data it was determined that about 80% of the ATP was metabolically active (Table 1). This results in a metabolic ATP pool of 12 nmol · mg protein^{-1}. From similar measurements it was calculated that the retinal content of metabolic orthophosphate was 15 nmol · mg protein^{-1} (viz., 25% of 60 nmol · mg protein^{-1} orthophosphate was metabolic). If the metabolic ATP and the metabolic orthophosphate share the same compartment, then β is equal to (15 nmol · mg protein^{-1})/(12 nmol · mg protein^{-1}) or 1.25. With w^* set to 0.428 and β set to 1.25, the value for parameter α of the gamma model was varied to fit the data. A value of 30 s for α was used to generate the three theoretical curves in Fig. 3; the curves correspond to the fractions of ATP in the metabolic pool that have one, two, or three atoms of ^{18}O in the γ-phosphoryl. Since the effect of varying α is to rescale the curves along the time-axis (see Discussion), the value of α that provides the best fit of the gamma model to the data, by any criterion, must be on the order of 30 s.

The time course of the ^{18}O distribution in the

TABLE 2 Time course of ^{18}O incorporation into the γ-phosphoryl of ATP in dark-adapted, isolated toad retina at 22°C

	Time course of ^{18}O distribution over the entire pool of ATP			
Incubation time	$T_0/\bar{T}$	$T_1/\bar{T}$	$T_2/\bar{T}$	$T_3/\bar{T}$
s				
20	0.8866	0.0909	0.0207	0.0018
40	0.8424	0.1173	0.0364	0.0039
60	0.7828	0.1628	0.0470	0.0074
120	0.6208	0.2553	0.1025	0.0213
600	0.3360	0.3493	0.2344	0.0802
1800	0.2637	0.4004	0.2751	0.0609
3600	0.3318	0.3460	0.2584	0.0637
	Time course of ^{18}O distribution over the metabolic pool of ATP			
Incubation time	T'_0	T'_1	T'_2	T'_3
s				
20	0.86	0.11	0.025	0.0022
40	0.81	0.14	0.044	0.0048
60	0.74	0.20	0.057	0.0090
120	0.54	0.31	0.13	0.026
600	0.19	0.43	0.29	0.098
1800	0.10	0.49	0.34	0.074
3600	0.19	0.42	0.32	0.078

Procedure to convert fractions normalized to the entire ATP pool to fractions normalized to the metabolic ATP pool: divide all values for $T_1/\bar{T}$, $T_2/\bar{T}$ and $T_3/\bar{T}$ by $f_{metabolic}$ to obtain T'_1, T'_2, and T'_3, respectively; for each incubation time, set the value of T'_0 equal to $1 - T'_1 - T'_2 - T'_3$. For the above experiment, the metabolic pool of ATP was determined from the distribution of ^{18}O at isotopic equilibrium to be 82% of the entire ATP pool (Table 1); in otherwords, $f_{metabolic} = 0.82$. Data were collected from three retinas for the 40-s incubation time; the standard deviations (with $n = 3$) for $T_0/\bar{T}$, $T_1/\bar{T}$, $T_2/\bar{T}$, and $T_3/\bar{T}$ are, respectively, 0.0131, 0.0115, 0.0052, and 0.0007.

γ-phosphoryl of ATP and in orthophosphate of human platelets at 37°C are given in Table 3. The data, expressed in terms of fraction of metabolic pool, are plotted in Fig. 4. From the distribution of ^{18}O in the γ-phosphoryl of ATP at isotopic equilibrium, a value of 0.323 is obtained for w^* (Table 1). Values for parameters α and β of the gamma model were varied to fit the data. The curves shown in Fig 4, *A* and *B*, are generated with values $w^* = 0.323$, $\alpha = 0.9$ s, and $\beta = 20$. Values of α and β that differ significantly from these selected values will result in a poor fit to the data. In comparison to the example given with data from toad retinas, direct measurements of the contents of ATP and of orthophosphate in platelets were not required. However, in this case, a unique determination of α and β would not have been possible if only the γ-phosphoryl data in Fig. 4 *A* or only the orthophosphate data in Fig. 4 *B* had been available.

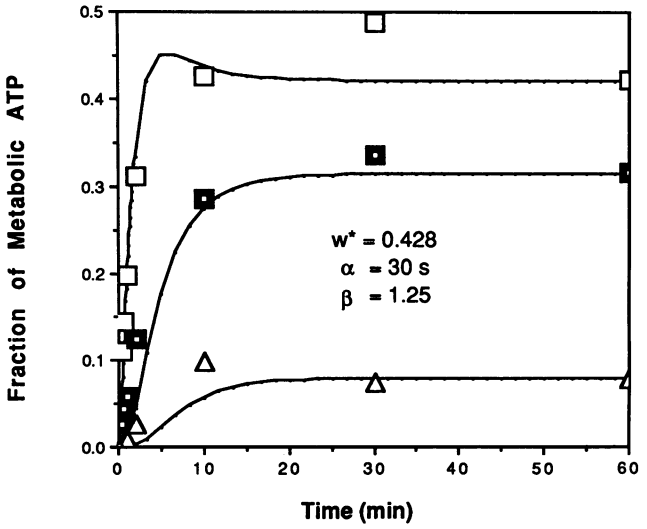

FIGURE 3 Time course of ^{18}O incorporation into the γ-phosphoryl of metabolic ATP in dark-adapted toad retinas at 22°C. The experimental data have been normalized to display ^{18}O labeling in terms of fractions of the metabolic ATP pool (see conversion from $T_j/\bar{T}$ to T'_j in Table 2). The fractions of metabolic ATP containing one, two, or three atoms of ^{18}O in the γ-phosphoryl are shown by unfilled squares, filled squares, and unfilled triangles, respectively. The data are fitted by theoretical curves generated by the gamma model, Eqs. (7.1) to (7.15), with computations performed on a Macintosh II by STELLA with a dt = 0.125 s. The model has three degrees of freedom: (*a*) w^*, defined to be the fraction of intracellular water that is $H_2{}^{18}O$, (*b*) α, defined to be $1/k_{TD}$; and (*c*) β, defined to be $[\text{orthophosphate}_{\text{metabolic}}]/[\text{ATP}_{\text{metabolic}}]$. From the ^{18}O distribution at isotopic equilibrium it was determined that the intracellular water was enriched to 42.8% excess $H_2{}^{18}O$ (Table 1). From the isotopic equilibrium data the metabolic fractions of ATP and orthophosphate could be determined. These determinations were combined with measurements of total retinal contents of ATP and orthophosphate to calculate a value for β equal to 1.25. The specifications of w^* and β reduce the gamma model, in this case, to a single-parameter model. The value for the remaining parameter, α, was varied to obtain a fit to the data. The curves illustrated were obtained with an α of 30 s.

As pointed out above, the calculation of the size of the ATP metabolic pool is based on probabilities associated with the distribution of ^{18}O in the γ-phosphoryl of ATP whereas the calculation of ATP hydrolytic rate is additionally based on the kinetics diagrammed in Fig. 1 *A*. A degree of confidence in the calculations of the metabolic pool size is afforded by the close parallel between the values of the enrichment of intracellular water with $H_2{}^{18}O$, calculated from the modified binomial distribution, and the independently determined values of the enrichment of water in the incubation medium (Table 1). A partial assessment of the validity of using the gamma model to calculate the rate of ATP hydrolysis in intact cells is made in the next section.

The beta model

To the extent that the γ-phosphoryl of ATP and orthophosphate participate in rapid reactions not encompassed

TABLE 3 Time course of ^{18}O incorporation into the γ-phosphoryl of ATP and orthophosphate in human platelets at 37°C

	Time course of ^{18}O distribution over the metabolic pool of ATP			
Incubation time	T'_0	T'_1	T'_2	T'_3
s				
30	0.64	0.28	0.075	0.0074
60	0.49	0.37	0.13	0.015
180	0.35	0.43	0.20	0.030
360	0.31	0.44	0.21	0.034
600	0.31	0.44	0.21	0.033

	Time course of ^{18}O distribution over the metabolic pool of orthophosphate				
Incubation time	P'_0	P'_1	P'_2	P'_3	P'_4
s					
30	0.58	0.29	0.099	0.023	0.0043
60	0.49	0.32	0.15	0.039	0.0057
180	0.29	0.38	0.24	0.082	0.011
360	0.25	0.39	0.26	0.091	0.013
600	0.24	0.40	0.26	0.088	0.013

For this platelet experiment, it was determined from the ^{18}O distribution at isotopic equilibrium that $f_{\text{metabolic}}$ for ATP is 0.57 (Table 1). This value for $f_{\text{metabolic}}$ was used to normalize the ATP data. It can be shown that for orthophosphate both the ratio of $P_1/\bar{P}$ to $P_2/\bar{P}$ (fractions normalized to entire pool) and the ratio of P'_1 to P'_2 (fractions normalized to metabolic pool) are equal to $2\{1\text{-}w^*\}/3w^*$. With this formula, the orthophosphate data yield a value of 0.299 for w^*. Similarly, from the ratio of doubly labeled to triply labeled orthophosphate, a value of 0.339 for w^* is obtained. The average w^* value of 0.319 given by these determinations coincides with the value of 0.323 determined from the ATP data (Table 1), supporting the validity of the modified binomial distribution. The value for $f_{\text{metabolic}}$ for orthophosphate, calculated from $f_{\text{metabolic}}$ (orthophosphate) $= (P_i/\bar{P})/4\{1\text{-}w^*\}^3w^*$, is 0.56. This value for $f_{\text{metabolic}}$ (orthophosphate) was used to normalize the orthophosphate data.

in Fig. 1 *A* the estimate of ATP hydrolytic rate based on the gamma model will be compromised. An independent estimate of the rate of ATP utilization under steady-state conditions can be obtained by monitoring the transfer of label between the β-phosphoryls of ADP to ATP. The basis of this method is the "beta model" schematically diagrammed in Fig. 1 *B*. It is assumed that an ^{18}O-labeled β-phosphoryl of ATP derives from an identically labeled β-phosphoryl of an ADP molecule which had been phosphorylated. The rate of synthesis of ATP from ADP is given by the flux, F_{DT}. In a steady state, the rate of utilization of ATP, denoted by F_T in Fig.1 *B*, must be equal to the rate of synthesis

$$F_{DT} = F_T \tag{8}$$

where F_{DT} and F_T have dimensions of concentration/time. It is not necessary to specify the various fates of ATP (e.g., hydrolysis to ADP, cleavage to AMP, conversion to cAMP, etc.). In particular, it is not necessary to know the rate at which labeled ATP is hydrolyzed to become labeled ADP. In the following analysis, the experimentally measured time course of the appearance of ^{18}O in the β-phosphoryl of ADP will serve as an "input" function to the beta model which will generate a theoretical time course of the labeling in the β-phosphoryl of ATP as an "output" function. Model parameters will be varied to fit this "output" function to experimental measurements of the time course of the labeling in the β-phosphoryl of ATP.

Some differences between the gamma and beta models should be noted. First, the flux determined by the beta model represents the sum of all rates of reactions in which ATP is utilized. By contrast, the gamma model is constructed to provide an estimate for the rate of ATP hydrolysis. Secondly, in theory, the beta model should be superior at estimating ATP utilization rate than the gamma model is at estimating ATP hydrolytic rate. For example, the occurrence of an ATP hydrolytic pathway with multiple reversals will result in an overestimate of ATP hydrolytic rate by the gamma model but will not affect the beta model. In short, the beta model is potentially superior to the gamma model because Fig. 1 B is more likely a closer approximation to the cellular reactions involving the β-phosphoryl of ATP than is Fig. 1 *A* to the reactions involving the γ-phosphoryl of ATP and orthophosphate. Unfortunately, as will be shown below, the temporal resolution of the beta model is poorer than that of the gamma model.

Given the steady-state Eq. (8), it can be derived from the system in Fig. 1 *B* that

$$d(bT'_j)/dt = \rho(bD'_j - bT'_j) \quad \text{for } j = 0, 1, 2, \text{ or } 3, \tag{9}$$

where bT'_j = the fraction of ATP in the "β-ATP metabolic pool" with j ^{18}O atoms in the β-phosphoryl at time t, bD'_j = the fraction of ADP in the "β-ADP metabolic pool" with j ^{18}O atoms in the β-phosphoryl at time t, $\rho = F_T/[b\text{ATP}_{\text{metabolic}}]$, and $[b\text{ATP}_{\text{metabolic}}]$ = the concentration of

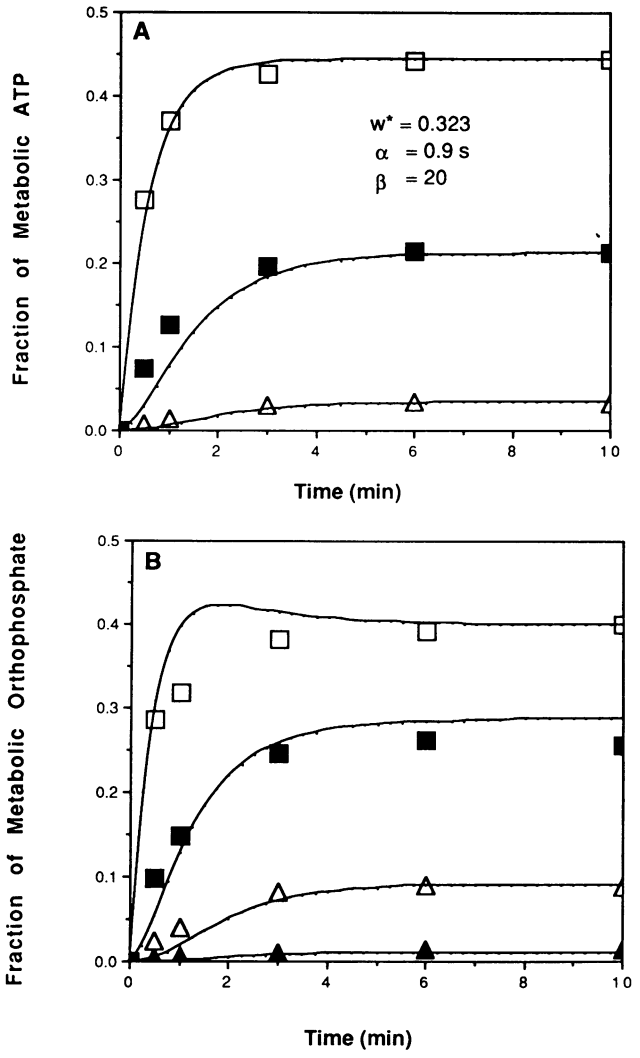

FIGURE 4 Time course of ^{18}O incorporation into the γ-phosphoryl of metabolic ATP and metabolic orthophosphate in human platelets at 37°C. The experimental data have been normalized to display ^{18}O labeling in terms of fractions of ATP and orthophosphate in the metabolic pool. (*A*) The fractions of metabolic ATP containing one, two, or three atoms of ^{18}O in the γ-phosphoryl are shown by unfilled squares, filled squares, and unfilled triangles, respectively. (*B*) The fractions of metabolic orthophosphate containing one, two, three, or four atoms of ^{18}O are shown by unfilled squares, filled squares, unfilled triangles, and filled triangles, respectively. The data are fitted by theoretical curves generated by the gamma model, Eqs. (7.1) to (7.15), with computations performed on a Macintosh II by STELLA with a dt = 0.0125 s. From the ^{18}O distribution at isotopic equilibrium it was determined that the intracellular water was enriched to 32.3% excess $H_2{}^{18}O$ (Table 1). This allowed the gamma model to be used as a two-parameter model. The values for α and β were varied to obtain a fit to the data shown in *A* and *B*. The curves illustrated were obtained with an α of 0.9 s and a β of 20.

ATP in the β-ATP metabolic pool. In the above definitions, the concept of metabolic pool is made specific for individual phosphoryls. The β-ATP metabolic pool refers to the pool of ATP molecules in which the β-phosphoryls are metabolized. Similarly, the β-ADP metabolic pool consists of ADP molecules with β-phosphoryls that are metabolized.

The solutions for Eq. (9) are given by the convolution integrals

$$bT'_j(t) = \rho \int_0^t bD'_j(\tau)e^{-\rho(t-\tau)}\,d\tau + bT'_j(0)$$

for $j = 0, 1, 2,$ or 3. (10)

(When the preparation is preincubated with medium lacking $H_2{}^{18}O$, the initial conditions are $bT'_0(0) = 1$ and $bT'_1(0) = bT'_2(0) = bT'_3(0) = 0$.) In Eq. (10), bD'_j serves as a temporal input function, bT'_j as a temporal output function, and ρ as a parameter of the model. Application of the Beta model to data introduces two additional parameters, $f_{\text{metabolic}}$ (bADP) and $f_{\text{metabolic}}$ (bATP), since the measured fractions of ^{18}O labeling must be normalized to the metabolic pool before the model can be applied.

A time course of incorporation of ^{18}O from $H_2{}^{18}O$ into the β-phosphoryl of ADP and ATP in human platelets is listed in Table 4. From the measurements made at 10 min, estimates for w^* can be calculated from the ratio of singly labeled to doubly labeled β-phosphoryls. Values of 0.308 and 0.316 are obtained from the ADP and ATP data, respectively. A plot of the data in Fig. 5 indicates that at 10 min isotopic equilibrium was not yet achieved

TABLE 4 Incorporation of ^{18}O into the β-phosphoryls of ADP and ATP in human platelets at 37°C

	Time course of ^{18}O distribution over the entire pool of ADP			
Incubation time	$bD_0/\bar{D}$	$bD_1/\bar{D}$	$bD_2/\bar{D}$	$bD_3/\bar{D}$
s				
30	0.9911	0.0068	0.0014	0.0005
60	0.9822	0.0132	0.0035	0.0009
180	0.9634	0.0253	0.0091	0.0019
360	0.9371	0.0421	0.0175	0.0032
600	0.9079	0.0601	0.0268	0.0049
	Time course of ^{18}O distribution over the entire pool of ATP			
Incubation time	$bT_0/\bar{T}$	$bT_1/\bar{T}$	$bT_2/\bar{T}$	$bT_3/\bar{T}$
s				
30	0.9704	0.0225	0.0062	0.0009
60	0.9483	0.0388	0.0110	0.0016
180	0.8629	0.0952	0.0366	0.0055
360	0.7665	0.1547	0.0678	0.0111
600	0.6908	0.2013	0.0932	0.0151

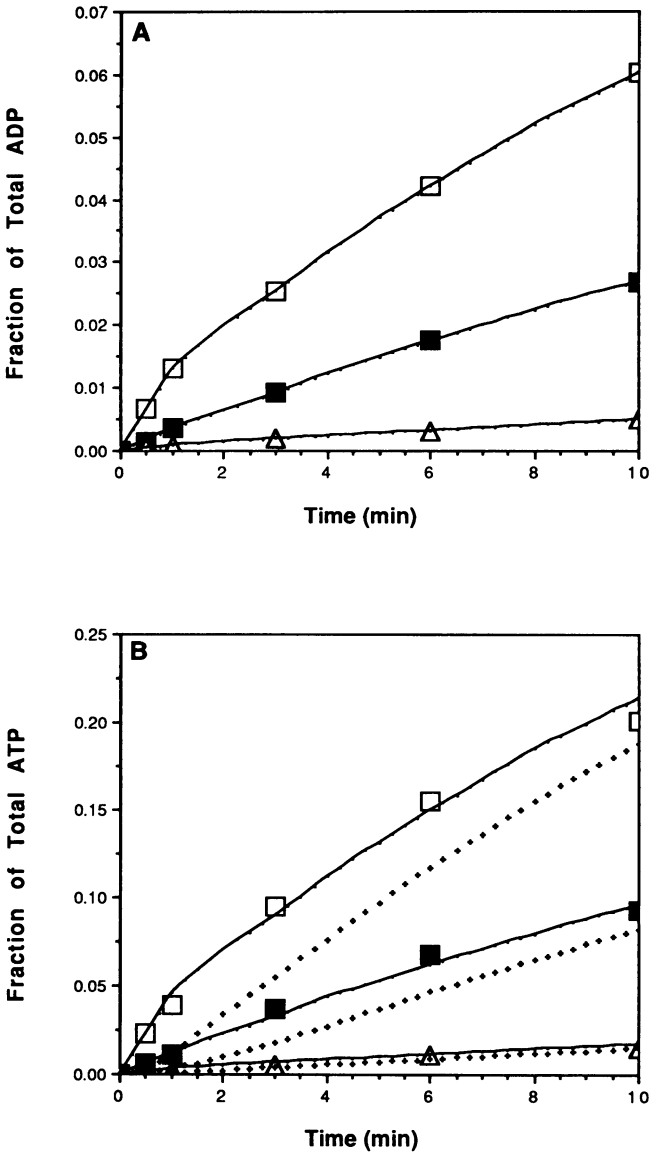

FIGURE 5 Time course of ^{18}O incorporation into the β-phosphoryls of (*A*) ADP and (*B*) ATP. The fractions of the total ADP pool or total ATP pool containing one, two, or three atoms of ^{18}O in the β-phosphoryl are shown by unfilled squares, filled squares, and unfilled triangles, respectively. The three continuous curves in *A* are interpolations of the measurements of ^{18}O in the β-phosphoryl of ADP. These curves were used as input functions for the beta model, given by Eq. (10), to generate output functions that correspond to the time course of ^{18}O incorporation into the β-phosphoryl of ATP. The continuous curves in *B* were generated in this manner by using the following parameter values: $f_{\text{metabolic}}$ (bADP) = 0.16; $f_{\text{metabolic}}$ (bATP) = 0.57, and ρ = 1 s. The $f_{\text{metabolic}}$ values were used to convert data format between "fraction of total pool" and "fraction of metabolic pool"; ρ is the time constant of ATP utilization. Any value of ρ equal to or less than 10 s will generate virtually the same curves shown for ρ = 1. The dotted lines are the output functions generated when ρ = 100 s. Therefore, the time constant of ATP utilization must be equal to or less than 10 s.

in the β-phosphoryls of the adenine nucleotides. By comparison the ^{18}O label in the γ-phosphoryl of ATP and orthophosphate had reached isotopic equilibrium by 10 min (Fig. 4). Therefore, the average value of 0.32 for w^* calculated from the ^{18}O distribution in these two groups (Tables 1 and 3, respectively) was used in the following calculations. From the formula $f_{metabolic}(bADP) = (bD_1/\bar{D})/3\{1 - w^*\}^2 w^*$ and a similar formula for $f_{metabolic}(bATP)$, tentative values of 0.14 and 0.45, respectively, were obtained from the data in Table 4 (10 min). Since isotopic equilibrium had not yet been attained in the β-phosphoryls by 10 min, the conclusion is that $f_{metabolic}(bADP)$ is greater than or equal to 0.14 and $f_{metabolic}(bATP)$ is greater than or equal to 0.45.

Since values for $f_{metabolic}(bADP)$ and $f_{metabolic}(bATP)$ could not be determined from the available data, these two values and a value for ρ had to be selected to fit the data with the beta model. There is no *a priori* reason for the β-ATP metabolic pool to be equal to the γ-ATP metabolic pool; however, as a starting point it was tentatively assumed that $f_{metabolic}(bATP) = 0.57$, the value of $f_{metabolic}$ obtained from the γ-phosphoryl of ATP (Table 1). The data in Fig. 5 *A* were interpolated by continuous curves, and these curves were rescaled by division by trial values of $f_{metabolic}(bADP)$ and used as input functions bD'_1, bD'_2, and bD'_3 to the beta model. Given trial values for ρ, the model (implemented by the STELLA program) generated output functions bT'_1, bT'_2, and bT'_3 corresponding to the three input functions. These output functions were renormalized to the entire ATP pool by multiplication by 0.57, the trial value for $f_{metabolic}(bATP)$, and compared with the ATP data in Fig. 5 B. With $f_{metabolic}(bATP)$ set to 0.57, the data in Fig. 5 *B* could be fit only by setting $f_{metabolic}(bADP)$ to 0.16 and ρ to any value less than or equal to 10 s. The validity of these values for metabolic pool sizes is supported by examining the distribution of ^{18}O in the β-phosphoryl of ADP and ATP in a separate experiment in which human platelets were incubated for 45 min in medium containing $H_2{}^{18}O$. For these data, listed in Table 5, isotopic equilibrium had been reached and the values for w^* of 0.403, from the ADP data, and 0.415, from the ATP data, agree closely with the value of 0.408 obtained in Table 1. In Table 5, it is shown that the ^{18}O distribution in the β-phosphoryls of ADP and ATP is fit by the modified binomial distribution with $f_{metabolic}(bADP) = 0.19$ and $f_{metabolic}(bATP) = 0.62$. The latter value is equal to $f_{metabolic}$ determined for the γ-ATP metabolic pool (Table 1). Therefore, the tentative assumption made earlier that the β-ATP metabolic pool is equal to the γ-ATP metabolic pool is justified, and the result, from employing the beta model, that slightly less than 20% of the ADP belongs to the β-ADP metabolic pool is consistent with isotopic equilibrium data. Since the estimates for parameters $f_{metabolic}(bADP)$ and $f_{metabolic}(bATP)$ appear to be accurate, it can be concluded that the time constant of ATP utilization in human platelets at 37°C must be less than or equal to 10 s. Although the comparatively poor time resolution of the beta model does not permit a rigorous test of the validity of the gamma model, the results with the beta model suggest that the time constant of ~1 s for ATP hydrolysis obtained with the Gamma model is not unreasonable.

DISCUSSION

The models

The information presented indicates that the ^{18}O isotope tracer method can be used to determine the size of the ATP metabolic pool and the rate of ATP hydrolysis in intact cells. The γ-ATP metabolic pool size is determined by fitting the modified binomial distribution given by Eqs. (6.1) to (6.5) to the observed ^{18}O distribution in the γ-phosphoryl of ATP at isotopic equilibrium. The determination of metabolic pool size is independent of kinetic

TABLE 5 Application of the modified binomial distribution to measurements of ^{18}O in the β-phosphoryls of ADP and ATP in platelets incubated for 45 min in medium containing 43.9% $H_2{}^{18}O$

^{18}O distribution in the β-phosphoryls of ADP and ATP	Theoretical system Eqs (6.1) to (6.5)	Theoretical distribution at isotopic equilibrium
$bD_0/\bar{D} = 0.8509$	$w^* = 0.408$,	0.8494
$bD_1/\bar{D} = 0.0816$	$f_{metabolic}(bADP) = 0.19$	0.0815
$bD_2/\bar{D} = 0.0551$		0.0562
$bD_3/\bar{D} = 0.0124$		0.0129
$bT_0/\bar{T} = 0.5193$	$w^* = 0.408$,	0.5086
$bT_1/\bar{T} = 0.2563$	$f_{metabolic}(bADP) = 0.62$	0.2660
$bT_2/\bar{T} = 0.1820$		0.1833
$bT_3/\bar{T} = 0.0424$		0.0421

In the above, "theoretical system" refers to equations that are formally equivalent to Eqs. (6.1) to (6.5), which specify the general form for the distribution of ^{18}O among three sites.

considerations since it is based on data collected when the system has attained isotopic equilibrium. The two (free) parameters of the model are w^*, defined to be the fraction of intracellular water that is $H_2{}^{18}O$, and $f_{metabolic}$, defined to be the fraction of the ATP pool in which γ-phosphoryls are metabolically active. The fraction $f_{metabolic}$ can be defined for other phosphoryl groups and orthophosphate. The value of $f_{metabolic}$ for a group with n exchangeable oxygen sites can be determined by fitting the appropriate data with a modified nth-order binomial distribution (for example, a modified fourth-order binomial distribution is used for orthophosphate). The validity of this method for determining $f_{metabolic}$ values is indicated by the consistency of the corresponding values determined for w^*. First, for a given tissue or cell suspension, while the $f_{metabolic}$ values of different phosphoryl groups may differ, the value for w^* is the same regardless of which group is used to calculate it. This is consistent with expectations since each $f_{metabolic}$ value should be specific to a particular phosphoryl group whereas the w^* value is specific to intracellular water. Examples mentioned before are the 10-min incubation of human platelets (w^* based on the γ-phosphoryl of ATP is 0.323, see Table 1; average w^* based on orthophosphate is 0.319, see Table 3; and w^* based on the β-phosphoryls of ADP and ATP are respectively 0.308 and 0.316, which can be calculated from data listed in Table 4) and the 45-min incubation of platelets (w^* based on the γ-phosphoryl of ATP is 0.408, see Table 1; w^* based on the β-phosphoryls of ADP and ATP are respectively 0.403 and 0.415, which can be calculated from the data in Table 5). Secondly, as shown in Table 1, the calculated values for w^* closely parallel the values of ^{18}O enrichment of the water in the media. (Why the values calculated for the percent ^{18}O enrichment of intracellular water are consistently a few percentage points less than the percent ^{18}O enrichment determined for the extracellular water has not been ascertained. It is likely that it may represent, at least in part, metabolic water produced during the incubation.)

The present work demonstrates that the distribution of ^{18}O at isotopic equilibrium is described by a modified binomial distribution. The converse is not necessarily true; that is, it is not always the case that if a distribution of ^{18}O in a particular phosphoryl can be described by a modified binomial distribution, the phosphoryl is at isotopic equilibrium. For example, in Table 4 the ^{18}O distribution in the β-phosphoryls of the adenine nucleotides at 10 min can be described by modified binomial distributions yet, as is clear in Fig. 5, these phosphoryls have not achieved isotopic equilibrium. The reason is that the labeling in these β-phosphoryls derives from the transfer of labeled γ-phosphoryls from ATP which have reached isotopic equilibrium by 4 min (Fig. 4). Another caveat is that the metabolic pool should not be arbitrarily identified with the free pool. For example, the metabolic pool measured by the ^{18}O method could consist of a bound pool that rapidly exchanges with a metabolically active free pool. Alternatively, the metabolically active species may be a protein-bound form (as is the case in substrate channeling). In this case, a free pool that rapidly exchanges with the metabolically active bound pool would be included in the measurement of the metabolic pool. A final consideration is that, in the context of the procedure based on labeling with ^{18}O, the term metabolic is specific to the phosphoryl group and not the nucleotide. For example, it is possible that a pool exists of ADP molecules that never metabolize their α- or β-phosphoryls yet are very active metabolically because they accept and donate a γ-phosphoryl. This species of ADP would not be identified as metabolic by the ^{18}O method. With these qualifications, the application of the modified binomial distribution to ^{18}O distribution at isotopic equilibrium provides an accurate method for quantifying the metabolic pool sizes of phosphoryl pools in intact cells.

The gamma model, given by Eqs. (7.1) to (7.15), can be utilized to estimate the rate of hydrolysis of ATP in intact cells. The rate of ATP hydrolysis is determined by fitting the gamma model to the time courses of ^{18}O incorporation into the γ-phosphoryl of ATP and orthophosphate or, alternatively, fitting the former time course and measuring the ratio of the concentrations of orthophosphate and ATP in the metabolic pool. Each of the three parameters w^*, α, and β of the gamma model has a special significance. The parameter w^* is defined to be the fraction of intracellular water labeled with ^{18}O. As mentioned above, the value for w^* can be determined precisely by fitting the modified binomial distribution to the distribution of ^{18}O labeling of the γ-phosphoryl of ATP or orthophosphate at isotopic equilibrium. The value of w^* determines the values approached by the curves in Figs. 3, 4, and 5 as time increases. The parameter α is defined in Eq. (7.12) to be the inverse of k_{TD}, the rate constant of ATP hydrolysis (or, more generally, by Eq. (11.11) to be the ratio $[ATP_{metabolic}]/F$, where $[ATP_{metabolic}]$ is the concentration of ATP in the metabolic pool and F is equal to the ATP hydrolytic flux under steady-state conditions). Therefore, α is equal to the time required to hydrolyze an amount of ATP equal to the entire ATP content in the metabolic pool. If $[ATP_{metabolic}]$ is known, then the rate of ATP hydrolysis can be calculated since it is equal to the quantity $[ATP_{metabolic}]/\alpha$. Intuitively, the incorporation of ^{18}O into orthophosphate and the γ-phosphoryl of ATP should proceed faster for a large versus a small rate constant of ATP hydrolysis. This relationship can be readily seen in Eqs. (7.1) to (7.9). In this set of equations, α appears in all of the time derivatives and nowhere else; therefore the effect of α is to rescale the time axis—the smaller α is, the faster the rate

of ^{18}O incorporation will be. From Eq. (7.12), α is small when k_{TD} is large, that is, when the rate constant of ATP hydrolysis is high. Consequently, the equations express the idea that the rate of ^{18}O incorporation into orthophosphate and the γ-phosphoryl of ATP is directly proportional to the rate of ATP hydrolysis. A less obvious property of the gamma model expressed by the set of Eqs. (7.1) to (7.9) is that for a fixed rate of ATP hydrolysis the ^{18}O distribution characteristic of isotopic equilibrium will be approached faster when the ratio of [orthophosphate$_{metabolic}$] to [ATP$_{metabolic}$] is smaller. This occurs because, when [orthophosphate$_{metabolic}$]/[ATP$_{metabolic}$] is small rather than large, the orthophosphate pool becomes fractionally labeled more rapidly. In turn, upon rephosphorylation ADP has a greater chance to bond with a more highly labeled orthophosphate forming an ATP with a more highly labeled γ-phosphoryl. This feature can be seen in Eqs. (7.1) to (7.9) by noting that the third parameter of the model, β, is defined in Eq. (7.13) to be the ratio of [orthophosphate] to [ATP] in the metabolic pool. The parameter β appears only in the time derivatives of the fractional phosphate labeling in Eqs. (7.5) to (7.9). In a sense, β acts as an additional time scaling factor on the rate of ^{18}O incorporation by orthophosphate—the smaller the value for β, the faster the labeling rate of orthophosphate. β does not function solely in this manner since the fractions of labeled orthophosphate (P'_1, P'_2, P'_3, and P'_4) that it influences appear in Eqs. (7.1) to (7.4), which describe ^{18}O incorporation by the γ-phosphoryl of ATP. Therefore, the value for β will also affect the labeling rate of ATP (Appendix, third section). When attention is restricted to the time course of ATP labeling, the effect of a change in α to rescale the time course of ATP labeling can be counterbalanced by a change in β in the opposite direction. For this reason ATP data must be accompanied by the corresponding orthophosphate data in order to make a unique determination of α and β. In conclusion, each of the parameters w^*, α, and β embodies an important characteristic of the model.

The gamma model should be viewed as a first approximation to the kinetics of metabolism of the γ-phosphoryl of ATP. As shown in Figs. 3 and 4, the model provides a good description of the data with a minimum number of parameters. However, it appears to deviate consistently from the data in two ways. First, the model occasionally exhibits overshoots that are not evident in the data. Examples of such overshoots can be seen in the theoretical time courses of the fraction of metabolic ATP containing one atom of ^{18}O in the γ-phosphoryl, in Fig. 3, and of the fraction of metabolic orthophosphate containing one atom of ^{18}O, in Fig 4 *B*. Secondly, it seems that the gamma model initially underestimates the fractions of species containing more than one atom of ^{18}O (Figs. 3 and 4). Certainly, it will be possible to obtain better approximations to the data by increasing the complexity of the model. However, it must be determined whether the fit is improved because the refined model is more valid than the gamma model or simply because the number of degrees of freedom of the model has been increased. The usefulness of the gamma model is that (*a*) it is the simplest model that explains the incorporation of ^{18}O in the γ-phosphoryl of ATP and orthophosphate, (*b*) it gives an accurate estimate of ATP hydrolytic rate, provided that the reactions in Fig. 1 *A* are the overwhelmingly fastest reactions in which the γ-phosphoryl of ATP and orthophosphate are involved, and (*c*) it serves as a framework for future modeling.

To be meaningful, future refinements of the gamma model must be accompanied by additional types of observations. For example, one refinement will be to include phosphocreatine and the γ-phosphoryl of GTP in the theoretical model (Fig. 6 *A*) and to make the corresponding experimental observations of ^{18}O incorporation into these phosphoryls. With the inclusion of these phosphoryls, the model would account for the most rapid modes of ^{18}O incorporation. In fact, a partial assessment of the validity of the gamma model can be made by evaluating the potential magnitudes of contributions of these phosphoryls to ^{18}O labeling that presently are not taken into account. Platelets do not contain phosphocreatine, and the abundance of guanine nucleotides in platelets is one-eighth that of adenine nucleotides (Holmsen, 1985). Therefore, the estimate of ATP hydrolytic rate in platelets by the gamma model is not seriously compromised on this basis. In contrast, the toad retina contains a phosphocreatine pool that is ~1.7 times larger than the ATP pool. The gamma model does not account for ^{18}O-labeled γ-phosphoryls of ATP that are transferred to creatine. Maximal distortion would result if the rate of exchange between the γ-phosphoryl of ATP and phosphocreatine greatly exceeded the rate of ATP hydrolysis. This is the case, for example, in isolated rat heart (Bittl and Ingwall, 1985). If this is also true in the toad retina, the gamma model would overestimate the time constant for ATP hydrolysis by 2.7-fold since the calculated α would be equal to ([ATP$_{metabolic}$] + [PCr$_{metabolic}$])/(ATP hydrolytic flux) $\approx$ 2.7[ATP$_{metabolic}$]/(ATP hydrolytic flux) = 2.7/k_{TD}. (In addition, the parameter β would be equal to [orthophosphate$_{metabolic}$]/{[ATP$_{metabolic}$] + [PCr$_{metabolic}$]} rather than [orthophosphate$_{metabolic}$]/[ATP$_{metabolic}$].) In the toad retina, GTP is another possible source of error since the γ-phosphoryl of GTP incorporates ^{18}O as rapidly as the γ-phosphoryl of ATP (unpublished observations). Given that the retinal content of GTP is about one-third that of ATP, this pathway could, at maximum, lead to a 33% overestimate in the time constant of ATP hydrolysis. For the toad retina, the error introduced by ignoring the alternate pathways is slight since, in a second retina, a

A. High Flux Phosphoryl Reactions

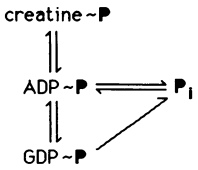

B. Multiple Reversal

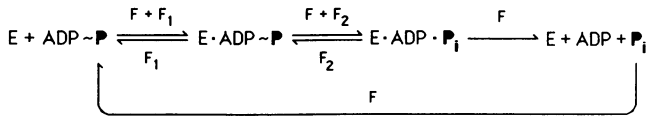

C. Compartmentation

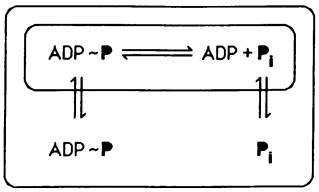

FIGURE 6 Possible refinements of the gamma model. (*A*) Reactions involving phosphoryls that rapidly incorporate ^{18}O from medium $H_2{}^{18}O$. The refined model takes into account ^{18}O-labeled γ-phosphoryls of ATP that are transferred to creatine or GDP instead of hydrolyzed. These phosphoryl transfer reactions can influence the calculation of the rate of ATP hydrolysis (see Discussion). The fluxes of ^{18}O-labeled phosphoryls through other pathways, such as adenylate kinase, are small in comparison with those diagrammed above, and therefore, can be ignored in models for the calculation of ATP hydrolytic rate. (*B*) A multiple-reversal model of ATPase activity. This model incorporates a simplified version of the kinetic model given by Bagshaw and Trentham (1973). An important modification is that the inorganic orthophosphate is recycled through the synthesis of ATP. Therefore, there are two modes by which phosphoryls become multiply labeled: recycling (flux F) and multiple reversal (flux F_2). A second key modification is that the release of ADP and inorganic phosphate from the ATPase is assumed to be irreversible in the intact cell (in cell-free preparations of myosin the reverse flux at this step is very slow and results in the exchange of oxygen between medium water and orthophosphate). Another multiple reversal model to be considered is one that involves a phosphoenzyme (see Boyer et al., 1977). The data may require a combination of these multiple reversal pathways with low and high exchange rates (Midelfort, 1981). However, it will be difficult to distinguish the effect of multiple reversal on ^{18}O incorporation from the effect of cellular compartmentation. (*C*) A simple model of compartmentation of ATP metabolism. This model is designed to explain the initial deviation of the gamma model from the observed time courses of multiply labeled species (Figs. 3 and 4). In this compartmentation model the appearance of multiply labeled species will be accelerated because the synthetic-hydrolytic recycling occurs in a small compartment. The highly labeled species slowly exchange with species in a larger compartment which by definition is part of the "metabolic pool." Therefore, species in the metabolic pool attain a high degree of multiple ^{18}O-labeling before the metabolic pool has become fully labeled.

calculation based on the sum of the early linear rates of ^{18}O incorporation into the γ-phosphoryls of ATP and GTP, orthophosphate, phosphocreatine, and the β-phosphoryls of ADP and ATP resulted in essentially the same time constant as that given by the gamma model applied to the data in Fig. 3.

Another possible refinement of the gamma model is to assign a nonzero probability to the event that the hydrolytic reaction undergoes reversal before the ATPase releases the ADP and orthophosphate products. A multiple reversal model is schematically diagrammed in Fig. 6 *B*. In this case, orthophosphate can become multiply labeled with ^{18}O before it is released by the enzyme. The most extensively studied example of this is the hydrolysis of ATP catalyzed by actomyosin (in slices of lobster muscle by Koshland and Clarke, 1953; in chemically skinned rabbit muscle by Hibberd et al., 1985; and in chemically skinned insect fibrillar muscle by Lund et al., 1987). Observations of exchange of ^{18}O label in cell-free preparations of myosin subfragment 1 or myosin have established that multiple labeling occurs by multiple reversal of the ATP hydrolytic reaction (Levy and Koshland, 1959; Shukla and Levy, 1977; Sleep et al., 1978). These studies also demonstrated that multiple reversals occur less often in the presence of actin and do not occur in medium containing Ca^{2+} at millimolar concentrations. Nevertheless, information is needed about the frequencies with which various ATPases undergo multiple reversals in the intact cell under physiological conditions. With multiple reversals, a single "functional" hydrolytic event can be associated with more than one incorporation of ^{18}O; if multiple reversals occur in the intact cell, the gamma model would underestimate the time constant of ATP hydrolysis. By analysis of the specific total ^{18}O labeling of the γ-phosphoryl of ATP and orthophosphate, it was determined that even with multiple reversals the time constant for ATP hydrolysis in the retina must be less than 55 s and for the platelet, less than 2.5 s.[3] With this

[3]The specific total labels in the γ-phosphoryl of ATP and in orthophosphate are defined in the Appendix by Eqs. (14.1) and (14.2), respectively. In the multiple-reversal model presented in the Appendix (fourth section), ξ is defined to be the average number of oxygens in the γ-phosphoryl of ATP that becomes exchanged with the oxygens of medium water. ξ is allowed to take on any value of 0 to 3, inclusive; the fourth oxygen in the product orthophosphate will derive from medium water as a result of the final hydrolytic cleavage. The multiple-reversal model also has parameters α, β, and w^*, which are defined similarly as for the gamma model. Although ξ is not restricted to integer values, it is informative to examine the effect of setting ξ to 0, 1, 2, or 3 on the choice of α. For the retina data listed in the lower half of Table 2, β was set to 1.25 and w^* was set to 0.428. The data could be fit with the following combinations of values for ξ and α: ($\xi = 0$, $\alpha = 18$ s); (1, 33 s); (2, 45 s); and (3, 55 s). Therefore, even if multiple reversals had exchanged all the oxygens in orthophosphate, the estimated time constant would be 55 s. With no multiple reversals ($\xi = 0$), an α is estimated to be 18 s. This is

analysis, which examines total ^{18}O labeling in each group, it is difficult to estimate the likelihood of multiple reversals. In theory, this estimation can be made by examining the distribution of ^{18}O within the γ-phosphoryl of ATP and orthophosphate. For example, a multiple reversal model could account for the deviation mentioned earlier between the gamma model and the initial time course of multiply labeled species. However, reversals cannot occur so often as to equilibrate all the oxygens in the γ-phosphoryl of ATP with the oxygens of medium water before its release from the ATPase as orthophosphate. Otherwise, with short incubation times the distribution of ^{18}O in orthophosphate and the γ-phosphoryl of ATP would be described by modified binomial distributions with the same w^*, but smaller $f_{metabolic}$ values, used to fit the data at isotopic equilibrium. In practice, it will be difficult to verify a multiple-reversal model for the intact cell. In the intact cell, the synthetic-hydrolytic cycle of ATP results in multiple labeling of orthophosphate. Therefore, the occurrence of multiply ^{18}O-labeled orthophosphate in intact cells is not *prima facie* evidence for the occurrence of multiple reversals. Neither is the initial deviation between model and data for multiply labeled species unequivocal evidence for multiple reversals since alternative explanations can be given.

One alternative explanation for the initial deviation between the gamma model and data is cellular compartmentation (Walseth et al., 1983). For example, the data can be explained with the model in Fig. 6 *C* in which (*a*) ATP hydrolysis is restricted to a small pool and (*b*) ATP and orthophosphate in the small pool is rapidly exchangeable with that of a larger pool. With this compartmentation model the ratio of multiply labeled species relative to singly labeled species in the total metabolic pool is initially elevated over that predicted by the gamma model because the distributions of ^{18}O in ATP and orthophosphate of the small hydrolytic pool rapidly approach binomial distributions. Clearly, the time constant calculated by the gamma model should not be interpreted as the time constant of a specific ATPase. It represents a weighted average of the time constants of hydrolysis of various ATPases and the time constants of exchange between ATP pools in the biological preparation. The present method based on labeling with ^{18}O (and for that matter, any other currently available method) of estimating *in situ* ATP hydrolytic rates does not resolve the component hydrolytic rates of ATP in different cell types in a tissue and in different cellular compartments within each cell. Consequently, it will not be easy to choose between a multiple reversal model and a compartmentation model. In conclusion, the gamma model represents a good first approximation to the data and serves as a foundation for further modeling. A more complete model will be developed to include cellular compartmentation and the high flux reactions involving the γ-phosphoryl of ATP. However, such theoretical refinements must be accompanied by the relevant experimental observations. In addition, the possibility that ATPases in intact cells undergo multiple reversals should be examined but will be difficult to prove.

In theory, the beta model, given by Eq. (10), can be used to make an accurate measurement of the time constant of ATP utilization under steady-state conditions. In practice, the time resolution of the beta model is poor and only an upper bound measurement of the time constant can be made. The reason for the limited time resolution is because the ^{18}O labeling of β-phosphoryls is much slower than that of γ-phosphoryls (viz. high-frequency components cannot be observed with a low-frequency input). On the other hand, the poor time resolution of the beta model indicates that *in situ* adenylate kinase activity is much slower than ATPase activity. Therefore, it is valid to ignore adenylate kinase in the scheme of Fig. 1 *A* (and Fig. 6 *A*) for estimating ATP hydrolytic rate.

Applications

From the distribution of ^{18}O in the γ-phosphoryl of ATP, it was determined that only 60% of the ATP in platelets is metabolically active (see Table 1). This finding is consistent with the observation that a significant amount of the adenine nucleotides in platelets is stored in secretory, dense granules (Holmsen, 1985; Ugurbil and Holmsen, 1981). The ATP in the storage pool is nonmetabolic and requires hours to exchange with the cytoplasmic pool of ATP (Reimers et al., 1975). From previous measurements (see Holmsen, 1985) it can be estimated that slightly more than half of the ATP in human platelets is in the cytoplasm.[4] Therefore, the present measurements suggest that in platelets, the entire cytoplasmic pool of

lower than the estimate of 30 s obtained in Fig. 3 because in fitting the graphical data the species containing one atom of ^{18}O was given maximum weighting (and consequently multiply labeled species were underestimated) whereas, in the multiple reversal model, the "specific total label" weights multiply labeled species heavily. For the platelet data in Table 3, β was set to 20 and w^* was set to 0.32. The data could be fit with the following combinations of values for ξ and α: (0, 0.6 s); (1, 1.1 s); (2, 1.7 s); and (3, 2.5 s).

[4]If the sum of cellular ATP and ADP accounts for essentially all of the total adenine nucleotides in the platelet, the compartmentation of ATP and ADP can be estimated from the ratios given by Holmsen (1985) to be: 30.3% of the total adenine nucleotides is cytoplasmic ATP; 3% is cytoplasmic ADP; 27.5% is ATP in the dense granules; and 39.2% is ADP in the dense granules. This distribution is in accordance with the reported ratios: two-thirds of the ADP and ATP are in the dense granules where the [ATP]/[ADP] ratio is 0.7, and the [ATP]/[ADP] ratio in the cytoplasm is 10. With the distribution, 52.4% of the ATP and 7.1% of the ADP is in the cytoplasm.

ATP is involved in high energy metabolism. It was also determined by ^{18}O labeling that in the platelet slightly less than 20% of the ADP is metabolically active with respect to β-phosphoryl transfer. From ratio measurements of the compartmentation of adenine nucleotides (Holmsen, 1985), it can be estimated that 7% of the ADP in the platelet is in the cytoplasm and 93% is stored in the dense granules.[4] Thus, the small size of the ADP metabolic pool determined by ^{18}O incorporation would be predicted if only the ADP in the cytoplasm were metabolic.[5] The quantitative discrepancy of 16–19% estimated to be metabolic *vs.* 7% estimated to be cytoplasmic could simply reflect differences in platelet preparations or in the methods of determination. In regard to the latter point, the determination of the size of the β-ADP metabolic pool from the ^{18}O distribution at isotopic equilibrium should be accurate (provided that exchange between ADP in the cytoplasm and dense granule is negligible over 10–45 min and that perchloric acid does not preferentially extract ADP from either the cytoplasm or the dense granules). The enzyme most likely to be involved in the incorporation of ^{18}O into the β-phosphoryls of ADP and ATP is adenylate kinase.

From the time course of ^{18}O incorporation into the γ-phosphoryl of ATP and a measurement of β (=1.25), the time constant, α, of ATP hydrolysis in dark-adapted toad retinas at 22°C was estimated to be 30 s (see Fig. 3). Given a total retinal ATP concentration of 15 nmol · mg retinal protein^{-1} · s^{-1} and that 82% of the retinal ATP belongs in the metabolic pool (Table 1), this time constant of 30 s yields an ATP hydrolytic rate of ~400 pmol · mg retinal protein^{-1} · s^{-1}. If it is assumed that 10% of the retinal weight is protein, this is equivalent to 40 μM ATP · s^{-1} averaged over the entire retina. This rate of ATP hydrolysis is in the appropriate range based on calculations of the rate required to sustain the dark current in the photoreceptor. Zuckerman and Weiter (1980) determined from measurements of oxygen consumption that the dark current accounts for most of the ATP utilization in the rod photoreceptor. They also calculated that in the isolated bullfrog retina at 22°C the rod dark current requires 1.2×10^{-16} mol ATP · rod^{-1} · s^{-1}. Since the volume of the rod photoreceptor is on the order of 2 pl, this represents a requirement of ~60 μM ATP · s^{-1} in the rod. This is comparable to the rate of 40 μM ATP · s^{-1} (averaged over the entire retina) estimated with the gamma model.

From measurements of ^{18}O incorporation into the α-phosphoryls of GDP and GTP, it has been determined that in dark-adapted toad retinas at 22°C cGMP is hydrolyzed and synthesized at a rate of ~2 pmol · mg retinal protein^{-1} · s^{-1} (Dawis et al., 1988). Since two molecules of ATP are required for the resynthesis of one molecule of cGMP from the hydrolytic product GMP, cGMP metabolism in the dark-adapted toad utilizes ATP at a rate of 4 pmol · mg retinal protein^{-1} · s^{-1}. This is equivalent to 1% of the rate of total retinal ATP utilization. Photic stimulation of the toad retina causes an intensity-dependent increase in cGMP metabolic rate which at maximum is more than 10-fold greater than the rate in the dark steady state (Dawis et al., 1988). In the toad retina, since illumination does not change the rate of ATP utilization (unpublished observations), cGMP metabolism when maximally stimulated by light accounts for 10% of the total ATP utilization. This high level of energy consumption is remarkable when one considers that ATP utilization is distributed throughout the retina whereas cGMP metabolism is largely confined to the 40% of the retina consisting of rod outer segments (if ATP utilization is uniformly distributed throughout the retina, then the maximally stimulated cGMP metabolic system would account for 25% of the rod outer segment ATP utilization rate).[6] The generally accepted view of phototransduction is that photostimulated cGMP hydrolysis serves to lower the intracellular concentration of cGMP which in turn causes the closure of cation channels in the plasma membrane (Stryer, 1986). From a bioenergetic perspective, it would be much more efficient for illumination to result in a suppression of guanylyl cyclase (rather than an activation of cGMP phosphodiesterase) if the objective is to lower the intracellular concentration of cGMP. Instead, photic stimulation of the vertebrate retina results in the activation of the entire cGMP metabolic system (Goldberg et al., 1983; Ames et al., 1986; Dawis et al., 1988), which occurs without a lowering of the cGMP level and, from the above accounting, is a very energy expensive process. The high energy expenditure for the cGMP metabolic response to light is consistent with the view that the light-stimulated cGMP system "drives" some as yet unidentified biochemical process involved in phototransduction (Goldberg et al., 1983).

The gamma model yields an estimate of ~1 s for the

[5]Half of the cytoplasmic ADP in platelets is bound to F-actin (Holmsen, 1985). These bound ADP molecules, unlike the ADP in the dense granules, are rapidly exchangeable with cytoplasmic ADP; the time constant of exchange is 10 s at 37°C (Daniel *et al.*, 1979). Consequently, if free ADP in the cytoplasm belongs to the β-ADP metabolic pool, then actin-bound ADP is also included in this pool. This may not always be the case. For example, in skeletal muscle, actin-bound ADP is not part of the β-ADP metabolic pool (Zeleznikar, R. J., Dawis, S. M., and Goldberg, N.D., unpublished observations). Daniel *et al.* (1979) point out that when platelets are activated the exchange rate of actin-bound ADP with free ADP is reduced by 70%. They attribute this to a change in state of actin from nonfilamentous in resting platelets to F-actin in activated platelets.

[6]The light-accelerated ATP utilization due to stimulated cGMP metabolism is thus very likely the basis of the "ouabain respiratory response" described by Kimble et al. (1980).

time constant of ATP hydrolysis in human platelets at 37°C. This estimate was made even though the earliest data point in Fig. 4 was measured at 30 s. The reason that this is possible is because the value of 20 for β is large. Thus, although the equivalent of one metabolic pool of ATP turns over in 1 s, it takes about 20 s for the equivalent of one metabolic pool of orthophosphate to turn over. The result is that the overall dynamics of ^{18}O labeling are slowed and the 1-s time constant for ATP hydrolysis can be measured with relatively long incubation times. In contrast to the present findings, Akkerman et al. (1983) obtained a time constant of 77s for ATP utilization in cyanide-pretreated human platelets at 37°C. In their study the rate of ATP utilization was measured by blocking glycolysis with 2-deoxy-D-glucose and glycogenolysis with D-gluconic acid-1,5-lactone and monitoring the time course of ATP disappearance. As pointed out by Chapman and Atkinson (1977), it is likely that methods that employ metabolic inhibitors underestimate the rate of ATP utilization because of interfering regulatory mechanisms. The much faster time constant of 1 s obtained by application of the gamma model is supported by the use of the beta model. With the beta model, which most probably is a theoretically complete model of ATP utilization, it is clear that the time constant of ATP utilization must be less than or equal to 10 s. In Fig. 5 *B*, the continuous curves give the output functions of the beta model when the time constant is 1 s. Essentially identical curves are generated when the time constant is 10 s or less. These theoretical curves fit the data well. By comparison, when a time constant of 100 s is used, the dotted curves are produced. These curves lie well below the experimental data. An attempt to compensate for the difference by decreasing the value of $f_{metabolic}(b\text{ADP})$ below 0.16 is restricted by the observation, stated earlier, that from the ^{18}O label at 10 min it can be determined that $f_{metabolic}(b\text{ADP})$ must be greater than or equal to 0.14. The only other way to compensate for the difference is to increase $f_{metabolic}(b\text{ATP})$ above 0.57, but this is precluded by the observation that, in human platelets, $f_{metabolic}(b\text{ATP})$ is equal to the value of $f_{metabolic}$ for the γ-phosphoryl of ATP. In conclusion, it can be stated with little qualification that the time constant of ATP utilization is less than 10 s and with some qualification that the time constant of ATP hydrolysis is about 1 s in resting human platelets under physiological conditions.

APPENDIX

A simplified version of the gamma model

The kinetic model diagrammed in Fig. 1 A contains more structure than is required to deal with steady-state behavior. In particular, the model has the features that (*a*) the rate of ATP hydrolysis is proportional to the concentration of metabolic ATP and (*b*) the rate of ATP synthesis is proportional to the product of the ADP and orthophosphate concentrations in the metabolic pool. Under steady-state conditions these features are never utilized since these concentrations are constant. Consequently, the model can be simplified by substituting the rate equations with the corresponding steady-state fluxes. A schematic diagram of the biochemical reactions with this view is given below.

$$\text{ATP} \underset{F_{DT}}{\overset{F_{TD}}{\rightleftharpoons}} \text{ADP} + \text{orthophosphate},$$

where F_{TD} = the hydrolytic flux of metabolic ATP and F_{DT} = the synthetic flux of metabolic ATP. The above kinetic model can be combined with the same probabilistic model describing ^{18}O incorporation and loss into orthophosphate and the γ-phosphoryl of ATP used in constructing the gamma model. The state equations are given by

$$[\text{ATP}_{\text{metabolic}}]dT'_0/dt = -F_{TD}T'_0 + F_{DT}(1.00\,P'_0 + 0.25\,P'_1) \quad (11.1)$$

$$[\text{ATP}_{\text{metabolic}}]dT'_1/dt = -F_{TD}T'_1 + F_{DT}(0.75\,P'_1 + 0.50\,P'_2) \quad (11.2)$$

$$[\text{ATP}_{\text{metabolic}}]dT'_2/dt = -F_{TD}T'_2 + F_{DT}(0.50\,P'_2 + 0.75\,P'_3) \quad (11.3)$$

$$[\text{ATP}_{\text{metabolic}}]dT'_3/dt = -F_{TD}T'_3 + F_{DT}(0.25\,P'_3 + 1.00\,P'_4) \quad (11.4)$$

$$[\text{orthophosphate}_{\text{metabolic}}]dP'_0/dt = F_{TD}\{1 - w^*\}\,T'_0 - F_{DT}P'_0 \quad (11.5)$$

$$[\text{orthophosphate}_{\text{metabolic}}]dP'_1/dt = F_{TD}(w^*T'_0 + \{1 - w^*\}\,T'_1) - F_{DT}P'_1 \quad (11.6)$$

$$[\text{orthophosphate}_{\text{metabolic}}]dP'_2/dt = F_{TD}(w^*T'_1 + \{1 - w^*\}\,T'_2) - F_{DT}P'_2 \quad (11.7)$$

$$[\text{orthophosphate}_{\text{metabolic}}]dP'_3/dt = F_{TD}(w^*T'_2 + \{1 - w^*\}\,T'_3) - F_{DT}P'_3 \quad (11.8)$$

$$[\text{orthophosphate}_{\text{metabolic}}]dP'_4/dt = F_{TD}w^*T'_3 - F_{DT}P'_4 \quad (11.9)$$

with the following definitions: T'_j = the fraction of metabolic ATP with j ^{18}O atoms in the γ-phosphoryl at time t, for j = 0, 1, 2, or 3; P'_k = the fraction of metabolic orthophosphate with k ^{18}O atoms at time t, for k = 0, 1, 2, 3, or 4; $[\text{ATP}_{\text{metabolic}}]$ = the concentration of metabolic ATP during the $H_2{}^{18}O$ incubation period; $[\text{orthophosphate}_{\text{metabolic}}]$ = the concentration of metabolic orthophosphate during the $H_2{}^{18}O$ incubation period; w^* = the fraction of intracellular water containing ^{18}O at time t; and $\{1 - w^*\}$ = the fraction of intracellular water containing ^{16}O at time t. Since it is assumed that the system is in a steady state, the hydrolytic flux F_{TD} and the synthetic flux F_{DT} must be equal to the same flux, which will be referred to as F. Mathematically, it is assumed that

$$F_{TD} = F_{DT} = F. \quad (11.10)$$

Eqs. (11.1) to (11.9) can be rearranged into a form identical to that of

Eqs. (7.1) to (7.9) by using the following definitions:

$$\alpha = [\mathrm{ATP}_{\mathrm{metabolic}}]/F \tag{11.11}$$

$$\beta = [\mathrm{orthophosphate}_{\mathrm{metabolic}}]/[\mathrm{ATP}_{\mathrm{metabolic}}] \tag{11.12}$$

The only difference between the two models is that in the definition of parameter α the first-order rate constant k_{TD} in Eq. (7.12) is replaced by a concentration to flux ratio in Eq. (11.11). In other words, the requirement for linearity is removed.

Estimation of ATP hydrolytic rate from measurements of ^{18}O in the γ-phosphoryl of ATP and orthophosphate at several points in time

In the Results, a graphical method of estimating parameter values of the gamma model was illustrated. In the following, formulas are derived that can be used to estimate the parameter values by numerical methods. Define the terms:

$$T_{\mathrm{label}}(t) = T'_1(t) + 2T'_2(t) + 3T'_3(t) \tag{12.1}$$

$$P_{\mathrm{label}}(t) = P'_1(t) + 2P'_2(t) + 3P'_3(t) + 4P'_4(t), \tag{12.2}$$

where $T'_j(t)$ is defined as the fraction of ATP in the metabolic pool with j ^{18}O atoms in the γ-phosphoryl for $j = 0, 1, 2,$ or 3, and $P'_k(t)$ is defined as the fraction of orthophosphate in the metabolic pool with k ^{18}O atoms for $k = 0, 1, 2, 3,$ or 4. To simplify the text, the symbol (t) will be deleted in the following. From Eqs. (7.2) to (7.4) and (7.6) to (7.9) it can be derived that

$$\alpha \mathrm{d}T_{\mathrm{label}}/\mathrm{d}t = -T_{\mathrm{label}} + 0.75P_{\mathrm{label}}$$

$$\alpha \mathrm{d}P_{\mathrm{label}}/\mathrm{d}t = \beta^{-1}T_{\mathrm{label}} - \beta^{-1}P_{\mathrm{label}} + \beta^{-1}w^*.$$

(The relationship (7.14) was used in the derivation of the second equation above.) With a change in time scale and a change in notation to matrix form, the pair of equations becomes

$$\mathrm{d}\mathbf{X}(t)/\mathrm{d}(t/\alpha) = \mathbf{A}\mathbf{X}(t) + \mathbf{B}$$

with the following definitions

$$\mathbf{X}(t) = \begin{bmatrix} T_{\mathrm{label}} \\ P_{\mathrm{label}} \end{bmatrix}, \quad \mathbf{A} = \begin{bmatrix} -1 & 0.75 \\ \beta^{-1} & -\beta^{-1} \end{bmatrix}, \quad \text{and } \mathbf{B} = \begin{bmatrix} 0 \\ \beta^{-1}w^* \end{bmatrix}$$

To diagonalize matrix **A**, the eigenvalues must be determined from the equation $\det(\lambda\mathbf{I} - \mathbf{A}) = 0$ where det is the determinant, λ is a complex variable, and **I** is the 2×2 identy matrix. The solution of this quadratic equation yields two eigenvalues given by

$$\lambda_1 = \frac{-(\beta + 1) - \sqrt{(\beta + 1)^2 - \beta}}{2\beta} \tag{12.3}$$

$$\lambda_2 = \frac{-(\beta + 1) + \sqrt{(\beta + 1)^2 - \beta}}{2\beta} \tag{12.4}$$

From these eigenvalues a transformation matrix **T** that diagonalizes matrix **A** can be obtained. The matrix **T** is given by

$$\mathbf{T} = \begin{bmatrix} 1 & -(1 + \beta\lambda_2) \\ -1 & 1 + \beta\lambda_1 \end{bmatrix}.$$

The inverse of **T** is given by

$$\mathbf{T}^{-1} = \frac{1}{\beta(\lambda_1 - \lambda_2)} \begin{bmatrix} 1 + \beta\lambda_1 & 1 + \beta\lambda_2 \\ 1 & 1 \end{bmatrix}.$$

It is easily verified that $\mathbf{T}(\mathbf{T}^{-1}) = (\mathbf{T}^{-1})\mathbf{T} = \mathbf{I}$. The identities $\det(\lambda\mathbf{I} - \mathbf{A}) = 0$, $\beta\lambda_1\lambda_2 = 1/4$, and $\beta(\lambda_1 + \lambda_2) = -(\beta + 1)$ are useful in verifying the matrix **T** diagonalizes matrix **A**:

$$\mathbf{T}\mathbf{A}(\mathbf{T}^{-1}) = \begin{bmatrix} \lambda_1 & 0 \\ 0 & \lambda_2 \end{bmatrix},$$

where λ_1 and λ_2 are the eigenvalues determined previously. From matrix multiplication it can be shown that $\mathbf{T}\mathrm{d}\mathbf{X}(t)/\mathrm{d}(t/\alpha) = \mathbf{T}\mathbf{A}\mathbf{X}(t) + \mathbf{T}\mathbf{B} = \mathbf{T}\mathbf{A}\mathbf{I}\mathbf{X}(t) + \mathbf{T}\mathbf{B} = \mathbf{T}\mathbf{A}(\mathbf{T}^{-1})\,\mathbf{T}\mathbf{X}(t) + \mathbf{T}\mathbf{B}$. In otherwords, $\mathrm{d}\mathbf{X}'(t)/\mathrm{d}(t/\alpha) = \mathbf{A}'\mathbf{X}(t) + \mathbf{B}'$ where $\mathbf{X}'(t) = \mathbf{T}\mathbf{X}(t)$, $\mathbf{A}' = \mathbf{T}\mathbf{A}(\mathbf{T}^{-1})$, and $\mathbf{B}' = \mathbf{T}\mathbf{B}$. Since $\mathbf{A}'$ is diagonal, the two differential equations simplify to a form:

$$\mathrm{d}y(t)/\mathrm{d}(t/\alpha) = \lambda y(t) + C, \text{ with initial condition } y(0) = 0.$$

The solution of the above equation is $y(t) = -C\lambda^{-1}\{1 - e^{\lambda t/\alpha}\}$. For the specific equations derived above the solutions are

$$T_{\mathrm{label}} - (1 + \beta\lambda_2)P_{\mathrm{label}} = w^*(1 + \beta\lambda_2)(\beta\lambda_1)^{-1}\{1 - e^{(\lambda_1 t/\alpha)}\} \tag{12.5.1}$$

$$-T_{\mathrm{label}} + (1 + \beta\lambda_1)P_{\mathrm{label}} = -w^*(1 + \beta\lambda_1)(\beta\lambda_2)^{-1}\{1 - e^{(\lambda_2 t/\alpha)}\} \tag{12.5.2}$$

where t = time of incubation in medium containing $H_2{}^{18}O$, w^* = the fraction of intracellular water containing ^{18}O, β = $[\mathrm{orthophosphate}_{\mathrm{metabolic}}]/[\mathrm{ATP}_{\mathrm{metabolic}}]$, and T_{label}, P_{label}, λ_1, and λ_2 are defined by Eqs. (12.1) to (12.4), respectively. Eqs. (12.5.1) and (12.5.2) can be rearranged to

$$T_{\mathrm{label}} = (1 + \beta\lambda_2)\,P_{\mathrm{label}} + w^*(1 + \beta\lambda_2)(\beta\lambda_1)^{-1}\{1 - e^{(\lambda_1 t/\alpha)}\} \tag{12.6.1}$$

$$T_{\mathrm{label}} = (1 + \beta\lambda_1)\,P_{\mathrm{label}} + w^*(1 + \beta\lambda_1)(\beta\lambda_2)^{-1}\{1 - e^{(\lambda_2 t/\alpha)}\}. \tag{12.6.2}$$

Given measurements of T_{label} and P_{label} at various times t, Eqs. (12.6.1) and (12.6.2) can be used with an optimization algorithm to estimate values for α and β. For this optimization, it should be noted that λ_1 and λ_2 are functions of β. (Also a value for w^*, which can be determined separately from the distribution of ^{18}O at isotopic equilibrium, is required.) On the other hand, if β is known, the equations can be rearranged to give

$$e^{(\lambda_1 t/\alpha)} = 1 - \beta\lambda_1\{T_{\mathrm{label}} - (1 + \beta\lambda_2)\,P_{\mathrm{label}}\}/w^*(1 + \beta\lambda_2) \tag{12.7.1}$$

$$e^{(\lambda_2 t/\alpha)} = 1 - \beta\lambda_2\{T_{\mathrm{label}} - (1 + \beta\lambda_1)\,P_{\mathrm{label}}\}/w^*(1 + \beta\lambda_1) \tag{12.7.2}$$

and an exponential curve fitting algorithm can be employed. In theory,

Eqs. (12.7.1) and (12.7.2) could be used to determine a value for α from measurements made at a single point in time; however, in practice, the calculations are too sensitive to variability in data to permit estimation based on a single time point. (Eq. (12.7.2) is less sensitive than Eq. (12.7.1) to experimental variability.)

Finally, if the concentration of ATP in the metabolic pool, $[ATP_{metabolic}]$, is known, then

$$\text{rate of ATP hydrolysis} = [ATP_{metabolic}]/\alpha \quad (12.8.1)$$

$$[\text{orthophosphate}_{metabolic}] = \beta[ATP_{metablic}]. \quad (12.8.2)$$

The dependence of the incorporation of ^{18}O into the λ-phosphoryl of ATP and orthophosphate on time and parameters w^*, α, and β

Eqs. (12.5.1) and (12.5.2) can be viewed as simultaneous equations of two unknowns T_{label} and P_{label}. These equations can be solved to give explicitly the dependence of T_{label} and P_{label} on time and the three parameters of the gamma model. The solutions are

$$T_{label} = w^*(1 + \beta\lambda_1)(1 + \beta\lambda_2)\beta^{-2}(\lambda_1 - \lambda_2)^{-1} \cdot \{\lambda_1^{-1}\{1 - e^{(\lambda_1 t/\alpha)}\} - \lambda_2^{-1}\{1 - e^{(\lambda_2 t/\alpha)}\}\} \quad (13.1)$$

$$P_{label} = w^*\beta^{-2}(\lambda_1 - \lambda_2)^{-1}\{\lambda_1^{-1}(1 + \beta\lambda_2) \cdot\{1 - e^{\lambda_1 t/\alpha)}\} - \lambda_2^{-1}(1 + \beta\lambda_1)\{1 - e^{(\lambda_2 t/\alpha)}\}\}, \quad (13.2)$$

where λ_1 and λ_2 are functions of β given by Eqs. (12.3) and (12.4). Eqs. (13.1) and (13.2) express the time course of T_{label} and P_{label} in terms of parameters w^*, α, and β. These equations can be viewed in terms of two turnover times:

$$\alpha = [ATP_{metabolic}]/(\text{rate of ATP hydrolysis}) \quad (13.3)$$

$$\delta = [\text{orthophosphate}_{metabolic}]/(\text{rate of ATP hydrolysis}). \quad (13.4)$$

Since the two turnover times are related by $\delta = \alpha\beta$, eigenvalues (12.3) and (12.4) can be rewritten:

$$\lambda_1 = \frac{-(\delta + \alpha) - \sqrt{(\delta + \alpha)^2 - \delta\alpha}}{2\delta} \quad (13.5)$$

$$\lambda_2 = \frac{-(\delta + \alpha) + \sqrt{(\delta + \alpha)^2 - \delta\alpha}}{2\delta} \quad (13.6)$$

Therefore, λ_1/α and λ_2/α, which are the rate constants in the exponential terms in Eqs. (13.1) and (13.2), are symmetrical in α and δ. The relative magnitudes of the coefficients of these exponential terms are dependent only on β, which can be viewed as the ratio of the two turnover times, δ/α.

A multiple-reversal model

A model for the effect of multiple reversals on the specific total labeling of the γ-phosphoryl of ATP and orthophosphate is given by

$$[ATP_{metabolic}]dT_{specific}(t)/dt = -FT_{specific}(t) + FP_{specific}(t)$$
$$[\text{orthophosphate}_{metabolic}]dP_{specific}(t)/dt$$
$$= 0.25(3 - \xi)FT_{specific}(t) - FP_{specific}(t) + 0.25(1 + \xi)F$$

where ξ = the average number of oxygens exchanged ($0 \le \xi \le 3$),

$$T_{specific}(t) = T_{label}(t)/3w^* \quad (14.1)$$

$$P_{specific}(t) = P_{label}(t)/4w^* \quad (14.2)$$

and $T_{label}(t)$, $P_{label}(t)$, w^*, $[ATP_{metabolic}]$, $[\text{orthophosphate}_{metabolic}]$, and F are as previously defined. The functions $T_{specific}(t)$ and $P_{specific}(t)$ define the specific total labeling of the γ-phosphoryl of ATP and orthophosphate, respectively.

The authors wish to thank Melinda J.C. Lee, Beth S. Kuehn, and Eric A. Butz for technical assistance and expert mass spectrometer analysis of ^{18}O, and the latter for computer advice; Ann G. O'Toole for maintaining an effective laboratory support system; Dr. Dwight A. Burkhardt for providing facilities to conduct the experiments on the retina; and Dr. Peter Dudley of the National Eye Institute for making available an infrared image converter.

This work was supported by grants EY04877, GM28818, and AM07203 from the United States Public Health Service and Minnesota Leukemia Research Fund. Dr. Heyman was a recipient of a fellowship from the University of Minnesota Graduate School and Dr. Deeg was a recipient of a fellowship from the Life and Health Insurance Medical Research Fund.

Received for publication 23 July 1988 and in final form 19 August 1988.

REFERENCES

Akkerman, J. W. N., G. Gorter, L. Schrama, and H. Holmsen. 1983. A novel technique for rapid determination of energy consumption in platelets. *Biochem. J.* 210:45–55.

Ames, A. III, T. F. Walseth, R. A. Heyman, M. Barad, R. M. Graeff, and N. D. Goldberg. 1986. Light-induced increases in cGMP metabolic flux correspond with electrical responses of photoreceptors. *J. Biol. Chem.* 261:13034–13042.

Bagshaw, C. R., and D. R. Trentham. 1973. The reversibility of adenosine triphosphate cleavage by myosin. *Biochem. J.* 133:323–328.

Bittl, J. A., and J. S. Ingwall. 1985. Reaction rates of creatine kinase and ATP synthesis in the isolated rat heart. A ^{31}P NMR magnetization transfer study. *J. Biol. Chem.* 260:3512–3517.

Boyer, P. D., L. deMeis, M. G. C. Carvalho, and D. D. Hackney. 1977. Dynamic reversal of enzyme carboxyl group phosphorylation as the basis of the oxygen exchange catalyzed by sarcoplasmic reticulum adenosine triphosphatase. *Biochemistry.* 16:136–140,

Brown, T., K. Ugurbil, and R. Shulman. 1977. ^{31}P nuclear magnetic resonance measurements of ATPase kinetics of aerobic *Escherichia coli* cells. *Proc. Nat. Acad. Sci. USA.* 74:5551–5553.

Chapman, A. G., and D. E. Atkinson. 1977. Adenine nucleotide concentrations and turnover rates. Their correlation with biological activity in bacteria and yeast. *Adv. Microb. Physiol.* 15:253–306.

Daniel, J. L., L. Robkin, L. Salganicoff, and H. Holmsen. 1979. Measurement of the nucleotide exchange rate as a determination of the state of cellular actin. *In* Motility in Cell Function. F. A. Pepe,

J. W. Swanger, and V. T. Nachmias; editors. Academic Press, Inc., New York. 459–462.

Dawis, S. M., R. M. Graeff, R. A. Heyman, T. F. Walseth, and N. D. Goldberg. 1988. Regulation of cyclic GMP metabolism in toad photoreceptors: definition of the metabolic events subserving photoexcited and attenuated states. *J. Biol. Chem.* 263:8771–8785.

Dawson, M., D. Gadian, and D. Wilkie. 1978. Muscular fatigue investigated by phosphorous nuclear magnetic resonance. *Nature (Lond.).* 274:861–866.

Goldberg, N. D., A. Ames, III, J. E. Gander, and T. F. Walseth. 1983. Magnitude of increase in retinal cGMP metabolic flux determined by ^{18}O incorporation into nucleotide α-phosphoryls corresponds with intensity of photic stimulation. *J. Biol. Chem.* 285:9213–9219.

Hackney, D. 1980. Theoretical analysis of distribution of $[^{18}O]P_i$ species during exchange with water. Application to exchanges catalyzed by yeast inorganic pyrophosphatase. *J. Biol. Chem.* 258:5320–5328.

Hackney, D., and P. Boyer. 1978. Evaluation of the partitioning of bound inorganic phosphate during medium and intermediate phosphate $\rightleftharpoons$ water oxygen exchange reactions of yeast inorganic pyrophosphatase. *Proc. Natl. Acad. Sci. USA.* 75:3133-3137.

Hibberd, M. G., M. R. Webb, Y. E. Goldman, and D. R. Trentham. 1985. Oxygen exchange between phosphate and water accompanies calcium-regulated ATPase activity of skinned fibers from rabbit skeletal muscle. *J. Biol. Chem.* 260:3496–3500.

Holmsen, H. 1985. Nucleotide metabolism of platelets. *Annu. Rev. Physiol.* 47:677–690.

Karl, D. M., and P. Bossard. 1985. Measurement and significance of ATP and adenine nucleotide pool turnover in microbial cells and environmental samples. *J. Microbiol. Methods.* 3:125–139.

Kimble, E. A., R. A. Svoboda, and S. E. Ostroy. 1980. Oxygen consumption and ATP changes of the vertebrate photoreceptor. *Exp. Eye Res.* 31:271–288.

Koshland, D. E., and E. Clarke. 1953. Mechanism of hydrolysis of adenosinetriphosphate catalyzed by lobster muscle. *J. Biol. Chem.* 205:917–924.

Lee, R., A. Lanir, and M. Clouse. 1987. Liver adenine nucleotide metabolism during ischemia and reperfusion of mice livers studied by phosphorous-31 nuclear magnetic resonance. *Invest. Radiol.* 22:479–483.

Levy, H. M. and D. E. Koshland. 1959. Mechanism of hydrolysis of adenosinetriphosphate by muscle proteins and its relation to muscular contraction. *J. Biol. Chem.* 234:1102–1107.

Lipmann, F. 1941. Metabolic generation and utilization of phosphate bond energy. *Adv. Enzymol.* 1:99–162.

Lowry, O., J. Passonneau, F. Hasselberger, and D. Schulz. 1964. Effect of ischemia on known substrates and cofactors of the glycolytic pathway in brain. *J. Biol. Chem.* 239:18–30

Lund, J., M. R. Webb, and D. C. S. White. 1987. Changes in the ATPase activity of insect fibrillar flight muscle during calcium and strain activation probed by phosphate-water oxygen exchange. *J. Biol. Chem.* 262:8584–8590.

Midelfort, D. F. 1981. On the mechanism of actomyosin ATPase from fast muscle. *Proc. Natl. Acad. Sci. USA.* 78:2067–2071.

Reimers, H. J., J. F. Mustard, and M. A. Packham. 1975. Transfer of adenine nucleotides between the releasable and nonreleasable compartments of rabbit blood platelets. *J. Cell Biol.* 67:61–71.

Shukla, K. K., and H. M. Levy. 1977. Mechanism of oxygen exchange in actin-activated hydrolysis of adenosine triphosphate by myosin subfragment 1. *Biochemistry.* 16:132–136.

Sleep J. A., D. D. Hackney, and P. D. Boyer. 1978. Characterization of phosphate oxygen exchange reactions catalyzed by myosin through measurement of the distribution of ^{18}O-labeled species. *J. Biol. Chem.* 253:5235–5238.

Stryer, L. 1986. Cyclic GMP cascade of vision. *Annu. Rev. Neurosci.* 9:87–119.

Ugurbil, K., and H. Holmsen. 1981. Nucleotide compartmentation: radioisotope and nuclear magnetic resonance studies. *In* Platelets in Biology and Pathology. 2nd edition. J. L. Gordon, editor. Elsevier/North-Holland Biomedical Press, Amsterdam. 147–177.

Walseth T. F., J. E. Gander, S. J. Eide, T. P. Krick, and N. D. Goldberg. 1983. ^{18}O labeling of adenine nucleotide α-phosphoryls in platelets. *J. Biol. Chem.* 258:1544–1558.

Walseth, T. F., R. M. Graeff, and N. D. Goldberg. 1988. Monitoring cyclic nucleotide metabolism in intact cells by ^{18}O labeling. *Methods Enzymol.* 159:60–74.

Winkler, B. 1981. Glycolytic and oxidative metabolism in relation to retinal function. *J. Gen. Physiol.* 77:667–692.

Zuckerman, R., and J. J. Weiter. 1980. Oxygen transport in the bullfrog retina. *Exp. Eye Res.* 30:117–127.